The isobar collisions at RHIC : a tool for precision studies

Jiangyong Jia

Nuclear Structure

High-energy heavy-ion collisions

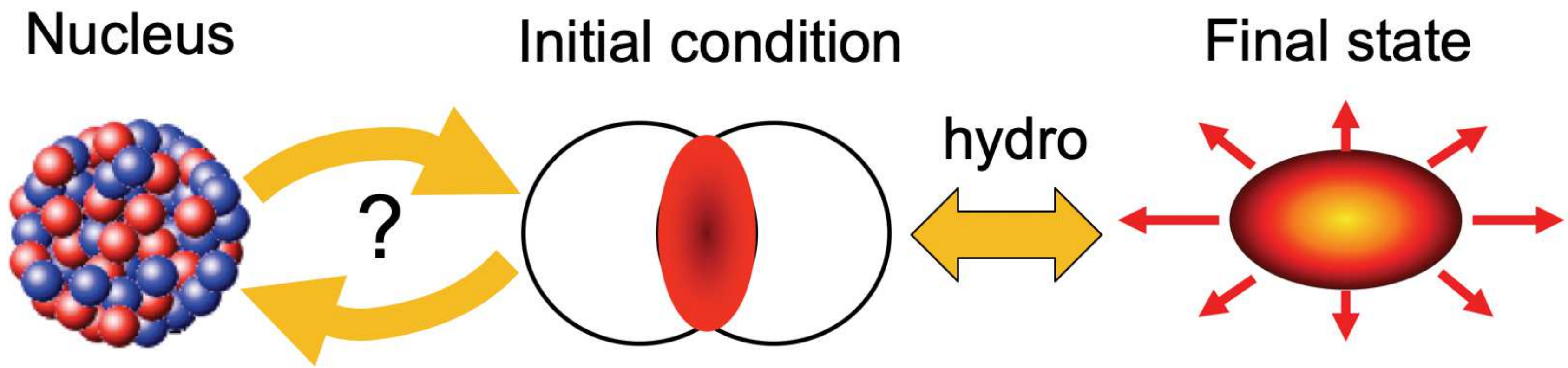

High-energy heavy ion collision

400 nucleons

$\tau < \frac{R}{\gamma} \approx 0.01\,\mathrm{fm}/c$

30,000 particles

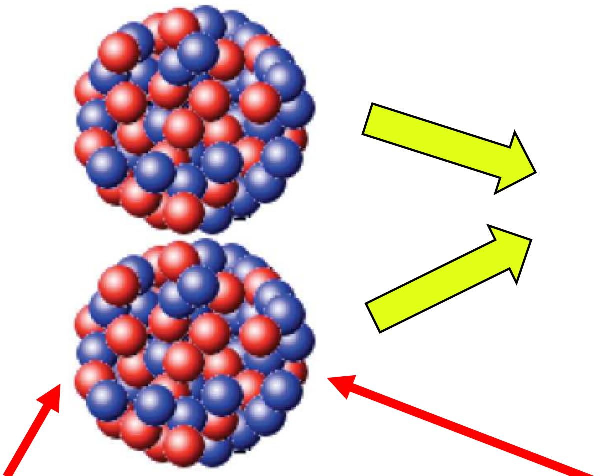

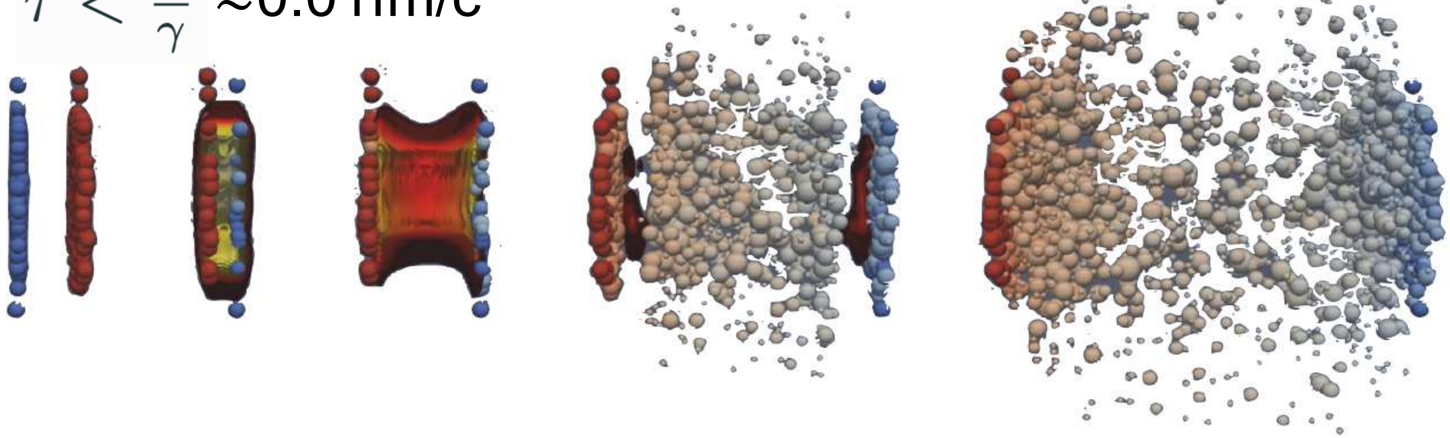

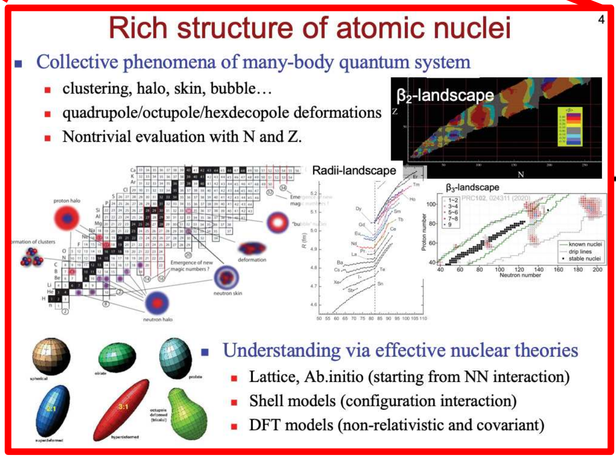

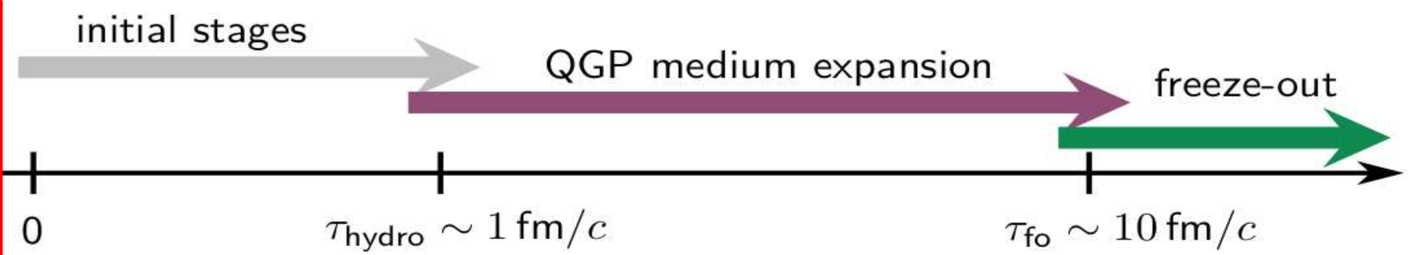

QGP response,
a smooth function of N+Z

Structure of colliding nuclei,
non-monotonic function of N and Z

Flow observable = k x f(initial condition)

Are HI probing the same thing as low-energy structure exp? Can HI provides competitive constraints on nuclear shape and radial profile?

From nuclear structure to Quark Gluon Plasma

Nucleus | Initial condition | Final state

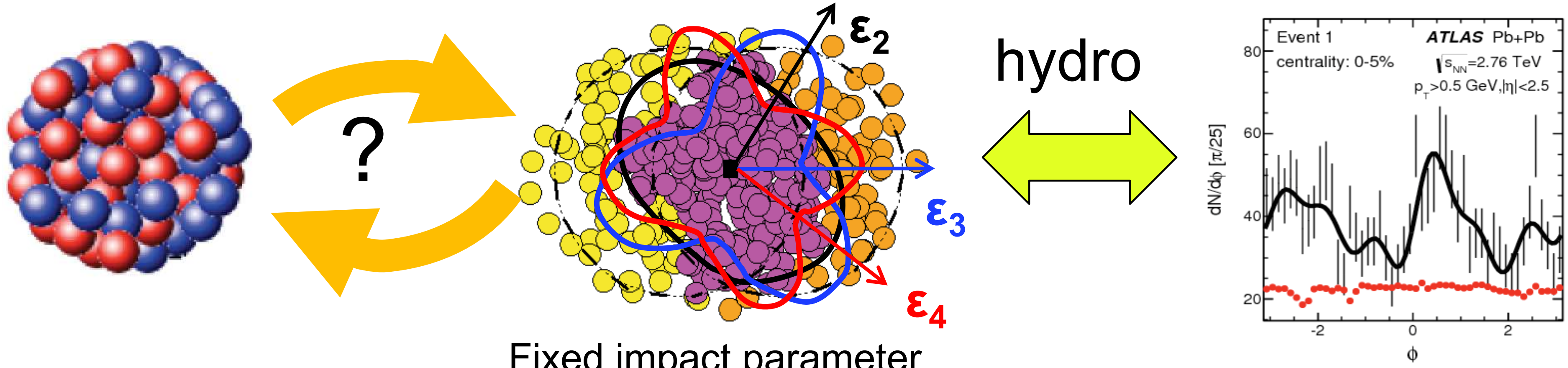

Fixed impact parameter

Shape-flow transmutation via pressure-gradient force:

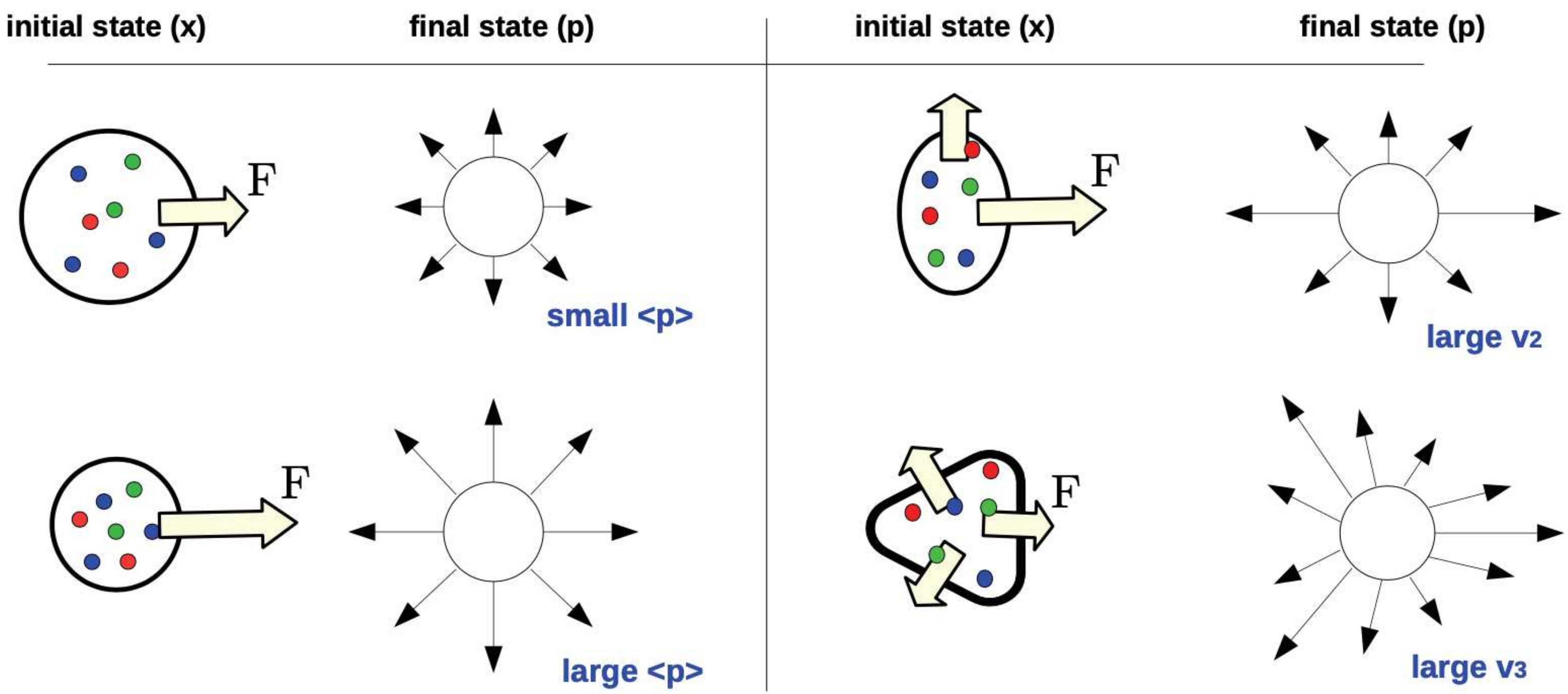

From nuclear structure to Quark Gluon Plasma

Nucleus

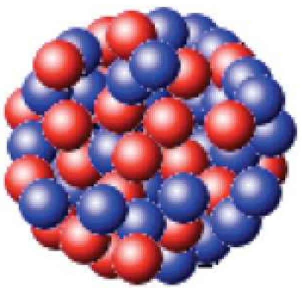

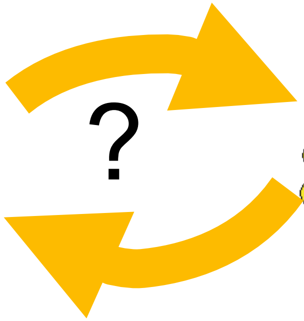

Initial condition

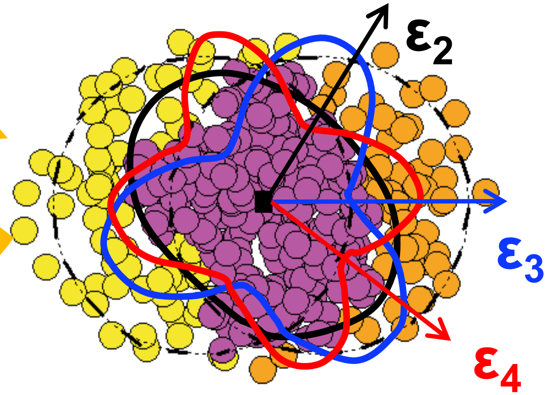

Fixed impact parameter

hydro

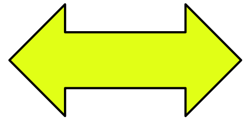

Final state

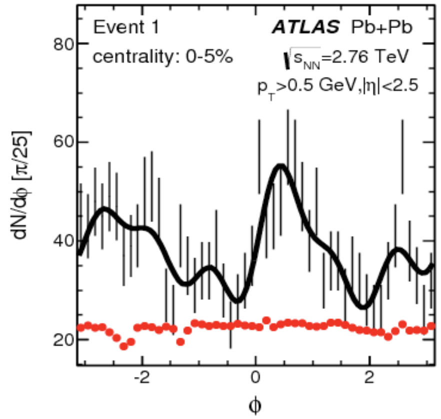

Nuclear structure	Initial volume	Initial Size	Initial Shape	Multiplicity	Radial Flow	Harmonic Flow

Nuclear structure

$$\rho(r,\theta,\phi) = \frac{\rho_0}{1+e^{(r-R(\theta,\phi))/a_0}}$$

$$R(\theta,\phi) = R_0\left(1+\beta_2[\cos\gamma Y_{2,0}+\sin\gamma Y_{2,2}] + \beta_3\sum_{m=-3}^{3}\alpha_{3,m}Y_{3,m} + \beta_4\sum_{m=-4}^{4}\alpha_{4,m}Y_{4,m}\right)$$

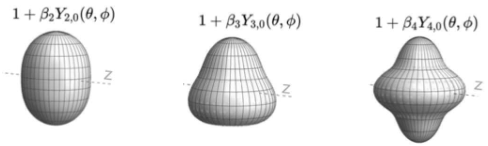

Triaxial spheroid: $a \neq b \neq c$.

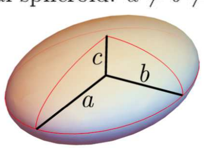

$0 \leq \gamma \leq \pi/3$

Initial volume: N_{part}

Initial Size: $R_\perp^2 \propto \langle r_\perp^2 \rangle$,

Initial Shape:

$$\mathcal{E}_2 \propto \left\langle r_\perp^2 e^{i2\phi}\right\rangle$$
$$\mathcal{E}_3 \propto \left\langle r_\perp^3 e^{i3\phi}\right\rangle$$
$$\mathcal{E}_4 \propto \left\langle r_\perp^4 e^{i4\phi}\right\rangle$$
$$\ldots$$

Multiplicity: N_{ch}

Radial Flow / Harmonic Flow:

$$\frac{d^2N}{d\phi dp_T} = N(p_T)\left(\sum_n V_n\, e^{-in\phi}\right)$$

High energy: approx. linear response in each event: $\tau < \frac{R}{\gamma}$

$$N_{ch} \propto N_{part} \qquad \frac{\delta[p_T]}{[p_T]} \propto -\frac{\delta R_\perp}{R_\perp} \qquad V_n \propto \mathcal{E}_n$$

Large event by-event analyzing power

Linear corr. between initial & final state

$$N_{ch} \propto N_{part}$$

$$\frac{\delta[p_T]}{[p_T]} \propto -\frac{\delta R_\perp}{R_\perp}$$

$$V_n \propto \mathcal{E}_n$$

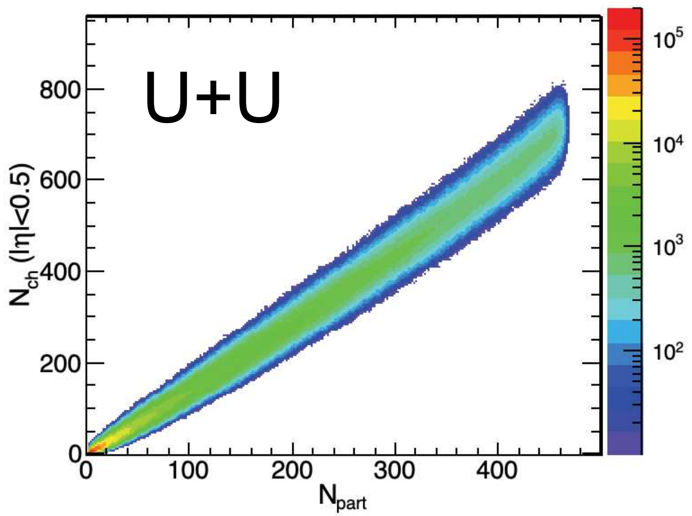

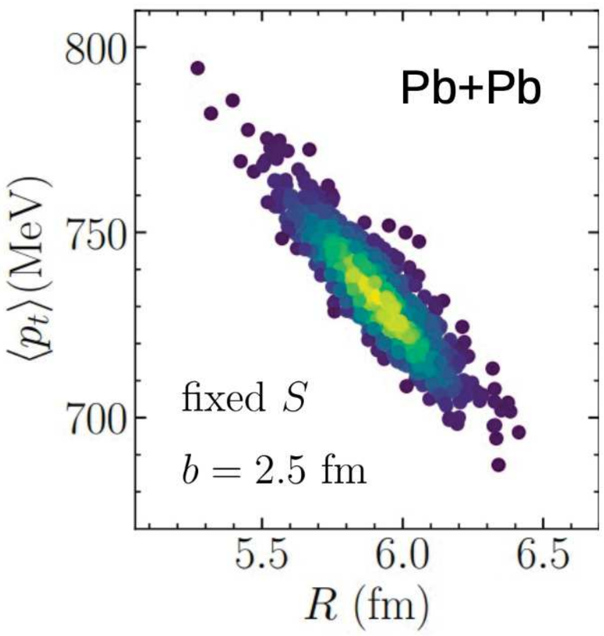

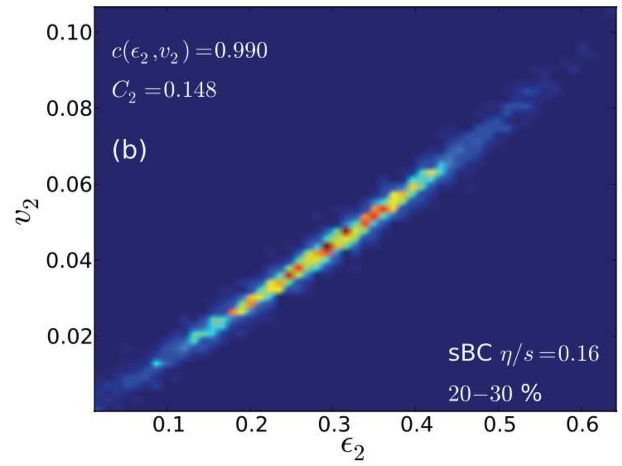

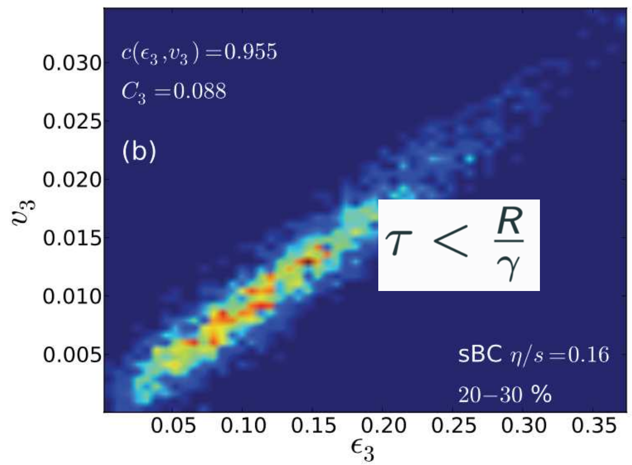

nice correlation at very high energy
breaks down at low energy

Long-range collective structure of nuclei

$$\rho(r,\theta,\phi) = \frac{\rho_0}{1+e^{(r-R(\theta,\phi))/a_0}}$$

$$R(\theta,\phi) = R_0\left(1+\beta_2[\cos\gamma Y_{2,0}+\sin\gamma Y_{2,2}]+\beta_3\sum_{m=-3}^{3}\alpha_{3,m}Y_{3,m}+\beta_4\sum_{m=-4}^{4}\alpha_{4,m}Y_{4,m}\right)$$

Quadrupole:

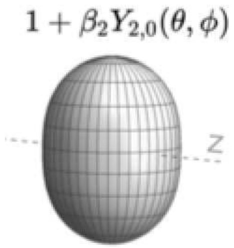

Octupole:

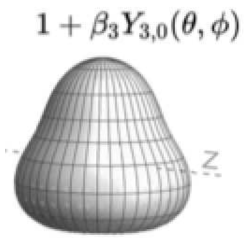

Hexadecapole:

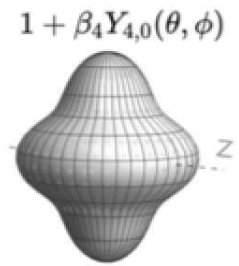

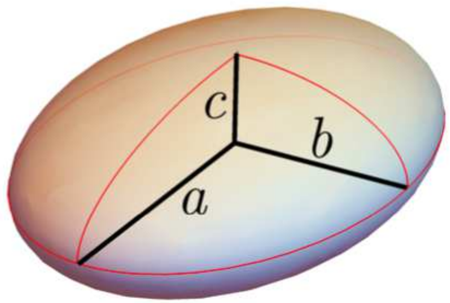

$0 \le \gamma \le \pi/3$

Prolate: a=b<c → β_2, $\gamma=0$

Oblate: a<b=c → β_2, $\gamma=\pi/3$

Triaxial: a<b<c → β_2, $\gamma=\pi/6$

How deformation influence HI initial state

Body-Body

$$\mathcal{E}_2 = \epsilon_2 e^{i2\Phi} \propto \left\langle \boldsymbol{r}_\perp^2 e^{i2\phi} \right\rangle$$

Tip-Tip

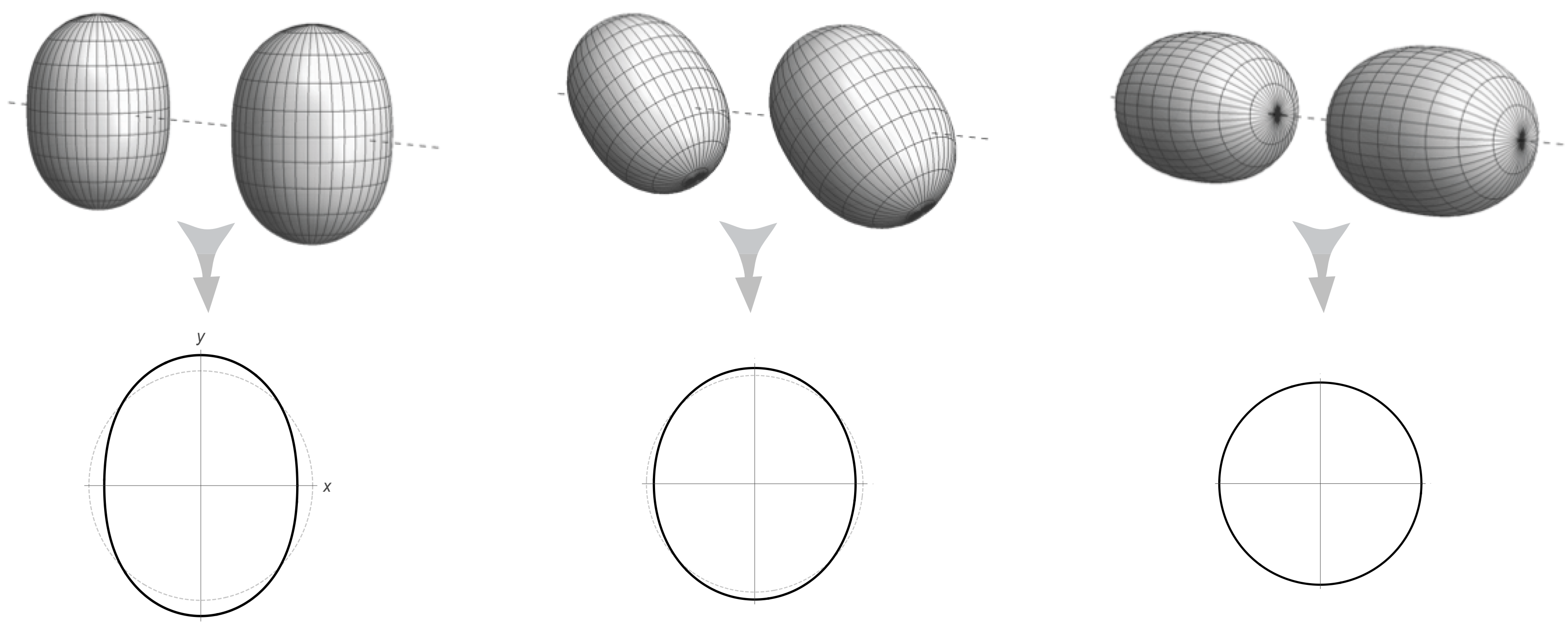

$\varepsilon_2 \sim 0.95\beta_2$

$\varepsilon_2 \sim 0.48\beta_2$

$\varepsilon_2 \sim 0$

$$\boldsymbol{\epsilon}_2 = \underbrace{\boldsymbol{\epsilon}_0}_{\text{undeformed}} + \underbrace{\boldsymbol{p}(\Omega_1, \Omega_2)}_{\text{phase factor}}\beta_2 + \mathcal{O}\left(\beta_2^2\right) \Longrightarrow \left\langle \epsilon_2^2 \right\rangle \approx \left\langle \epsilon_0^2 \right\rangle + 0.2\beta_2^2$$

Shape depends on Euler angle Ω=φθψ

How deformation influence HI initial state

- ε_n has the form $\epsilon_n = \underbrace{\epsilon_{n;0}}_{\text{undeformed}} + \sum_{m=2}^{4} \underbrace{\boldsymbol{p}_{n;m}(\Omega_1, \Omega_2)}_{\text{phase factor}} \beta_m + \mathcal{O}(\beta^2)$

$$\mathcal{E}_n = \epsilon_n e^{in\Phi} \propto \langle \boldsymbol{r}^2 Y_{n,n} \rangle$$

- $R_\perp^2 = \langle x^2 \rangle + \langle y^2 \rangle$ has the form $\delta d_\perp / d_\perp = \delta_d + \sum_{m=2}^{4} p_{0;m}(\Omega_1, \Omega_2)\beta_m + \mathcal{O}(\beta^2)$

  $d_\perp \equiv 1/R_\perp$

$$R_\perp^2 \propto \langle \boldsymbol{r}^2 Y_{2,0} \rangle$$

- Two particle correlation (two-body distribution)

$$\langle \varepsilon_n^2 \rangle \approx \langle \varepsilon_{n;0}^2 \rangle + \sum_m \langle \boldsymbol{p}_{n;m} \boldsymbol{p}_{n;m}^* \rangle \beta_m^2 \qquad \left\langle \left(\frac{\delta d_\perp}{d_\perp} \right)^2 \right\rangle \approx \langle \delta_d^2 \rangle + \sum_m \langle p_{0;m}^2 \rangle \beta_m^2$$

- In reality for medium size nucleus and ignore β_4.

$$\langle \varepsilon_2^2 \rangle = a_2' + b_2' \beta_2^2 + b_{2,3}' \beta_3^2 \quad \langle \varepsilon_3^2 \rangle = a_3' + b_3' \beta_3^2$$

$$\langle (\delta d_\perp / d_\perp)^2 \rangle = a_0' + b_0' \beta_2^2 + b_{0,3}' \beta_3^2$$

Glauber simulation

See 2106.08768

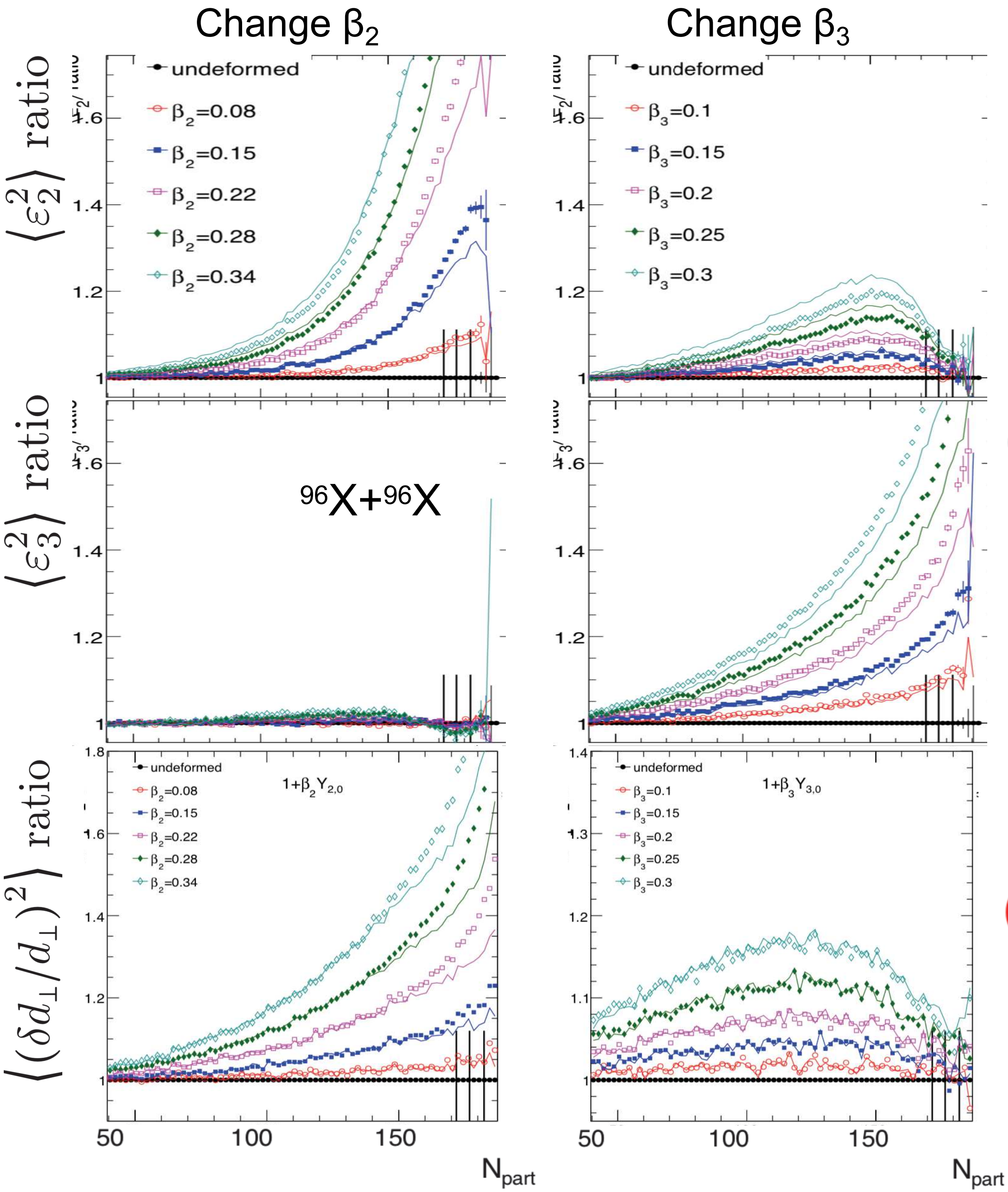

medium size system:

$$\varepsilon_2^2 = a_2' + b_2'\beta_2^2 + b_{2,3}'\beta_3^2$$

$$\varepsilon_3^2 = a_3' + b_3'\beta_3^2$$

$$(\delta d_\perp/d_\perp)^2 = a_0' + b_0'\beta_2^2 + b_{0,3}'\beta_3^2$$

$$v_2^2 = a_2 + b_2\beta_2^2 + b_{2,3}\beta_3^2$$

$$v_3^2 = a_3 + b_3\beta_3^2$$

$$(\delta p_{\mathrm{T}}/p_{\mathrm{T}})^2 = a_0 + b_0\beta_2^2 + b_{0,3}\beta_3^2$$

Application in ^{197}Au+^{197}Au vs ^{238}U+^{238}U

arXiv:2105.01638

Ultra-central Collisions at $\sqrt{s_{NN}}$=193-200 GeV

$$\begin{cases} v^2_{2,\mathrm{Au}} = a_{\mathrm{Au}} + b\beta^2_{2,\mathrm{Au}} \\ v^2_{2,\mathrm{U}} = a_{\mathrm{U}} + b\beta^2_{2,\mathrm{U}} \end{cases}$$

b~0.014

Need to correct for slightly different size: $a \propto 1/A\,,\quad r_a = \dfrac{a_{\mathrm{Au}}}{a_{\mathrm{U}}} = \dfrac{238}{197} = 1.21$

A linear relation for β_{2U} and β_{2Au} : $\beta^2_{\mathrm{U}} = \dfrac{r_{v_2^2} r_a - 1}{b/a_{\mathrm{U}}} + r_{v_2^2}\beta^2_{\mathrm{Au}} \qquad r_{v_2^2} = \dfrac{v^2_{2,\mathrm{U}}}{v^2_{2,\mathrm{Au}}}$

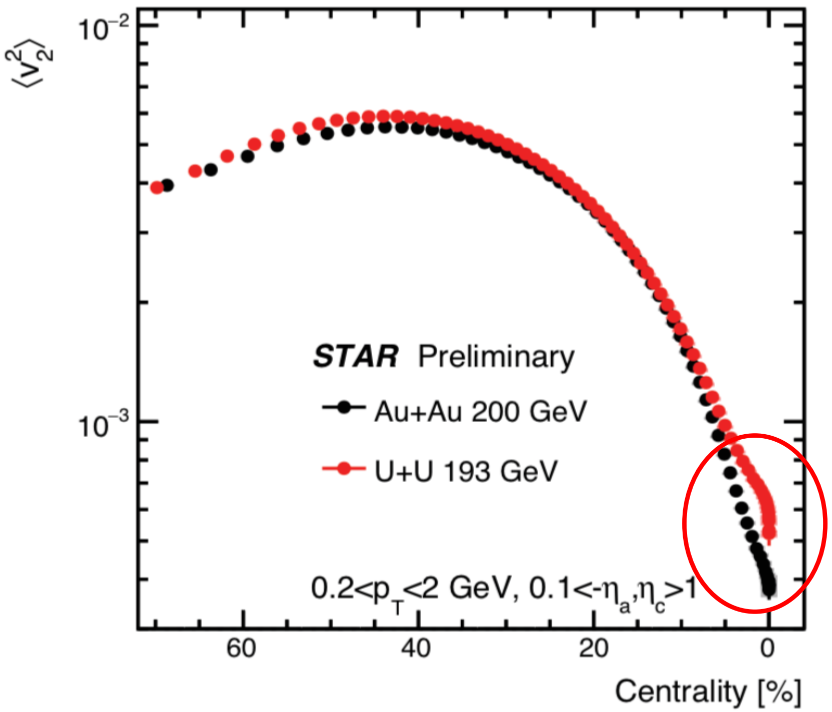

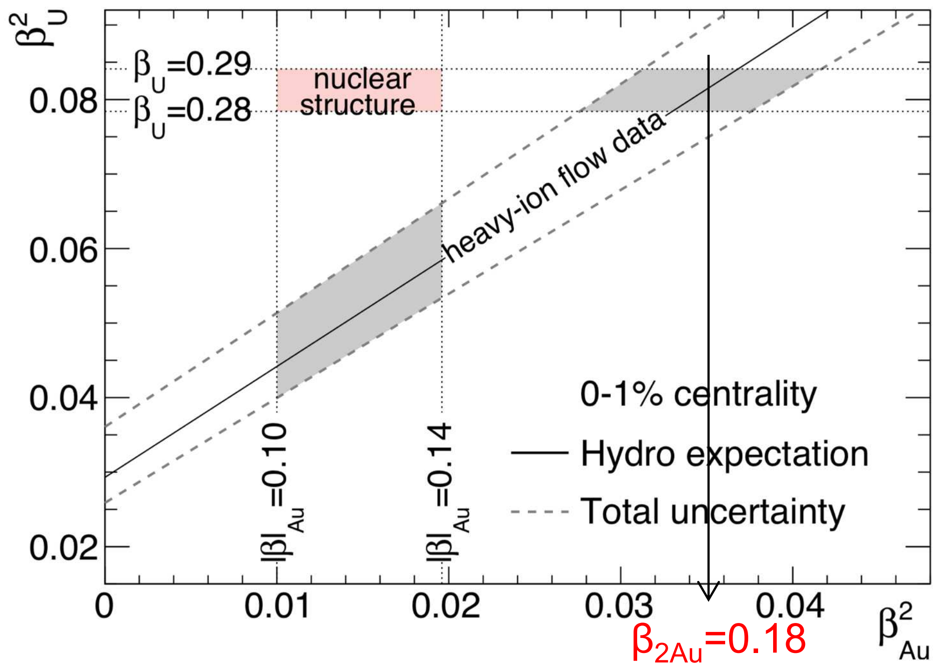

Suggests $|\beta_2|_{Au}$~0.18+-0.02, larger than NS model of 0.13+-0.02

But how to achieve precision?

Isobar collisions at RHIC: context

	Z	N	mass
96Ru	44	52	95.907598(8)
96Zr	40	56	95.908273(3)

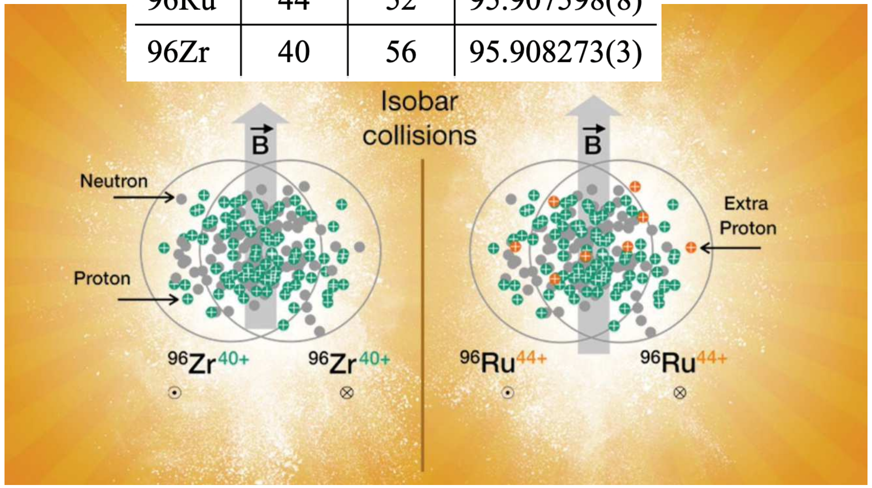

arXiv:2109.00131

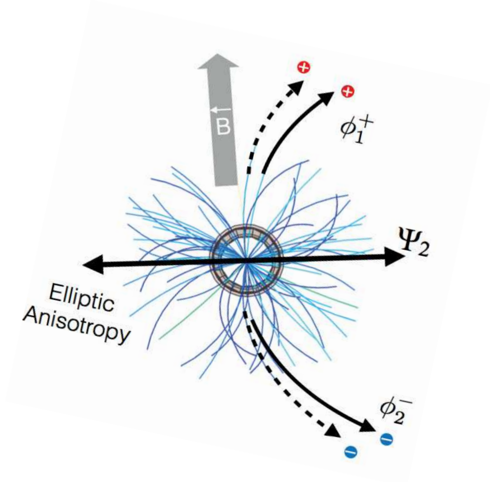

Voloshin, hep-ph/0406311

- Designed to search for the chiral magnetic effect: strong P & CP violation in the presence of EM field. Experimental signature is a spontaneous separation of + and - hadrons along EM direction, vertical to $\mathcal{E}_2$
- Turns out the CME signal is small, and isobar-differences are dominated by the nuclear structure differences.
- and turns out to be a precision tool for both NS physics & HI initial condition

Isobar collisions at RHIC/STAR

RHIC Running

From J Drachenberg

- Switch isobar species each time beam is inserted into RHIC
- Stable luminosity (matched between species) with long (~20 hour) beam circulation time
- Adjust and level luminosity to optimize data collection rate while minimizing backgrounds and systematics
- Restrict species-related information to those necessary for successful data-taking
- Calibration experts (recused from CME analyses) evaluate data quality “in real time”

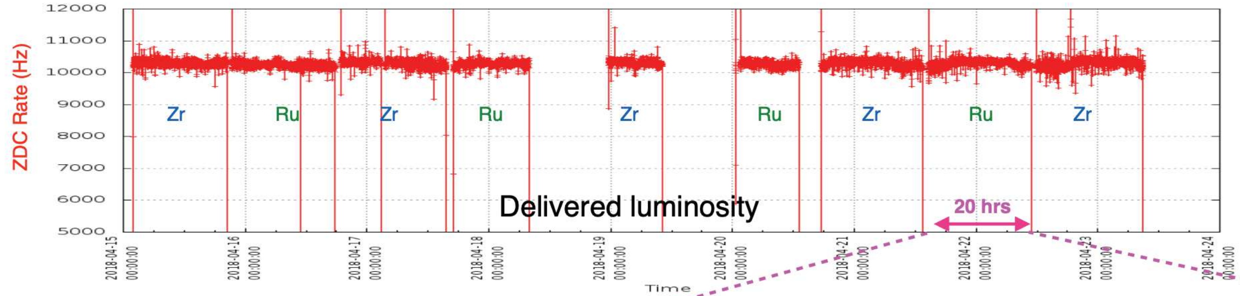

STAR : predefined blind analysis

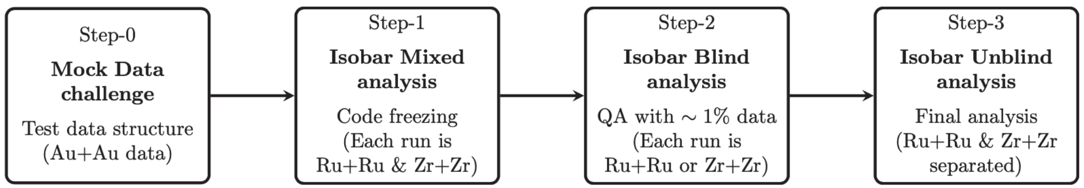

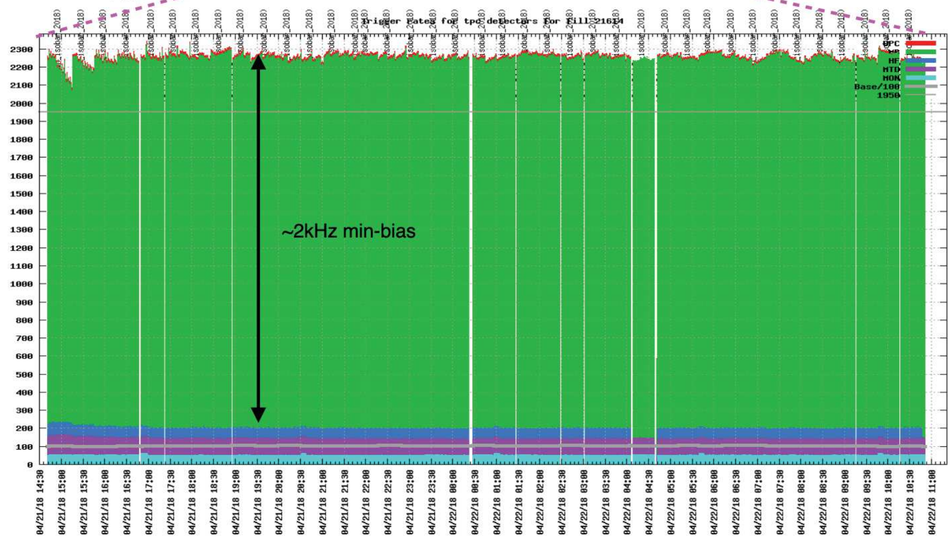

STAR Data Acquisition Rates

<0.4% precision is achieved in ratio of many observables between ^{96}Ru+ ^{96}Ru and ^{96}Zr+^{96}Zr systems→ precision imaging tool

Isobar collisions as a precision tool

- A key question for any HI observable O:

$$\boxed{\frac{O_{^{96}\mathrm{Ru}+^{96}\mathrm{Ru}}}{O_{^{96}\mathrm{Zr}+^{96}\mathrm{Zr}}} \stackrel{?}{=} 1}$$

Deviation from 1 must has origin in the nuclear structure, which impacts the initial state and then survives to the final state.

- Expectation

$$\rho(r,\theta,\phi) \propto \frac{1}{1+e^{[r-R_0(1+\beta_2 Y_2^0(\theta,\phi)+\beta_3 Y_3^0(\theta,\phi))]/a_0}}$$

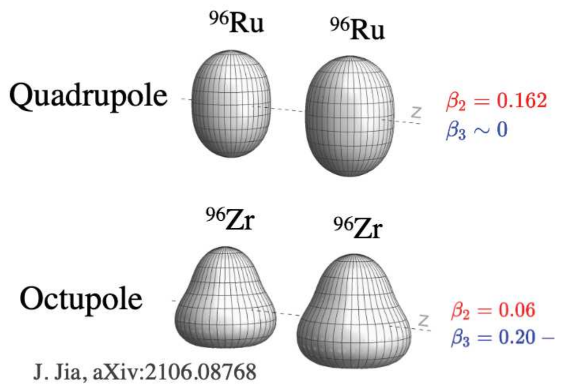

J. Jia, aXiv:2106.08768

$$\mathcal{O} \approx b_0 + b_1\beta_2^2 + b_2\beta_3^2 + b_3(R_0 - R_{0,\mathrm{ref}}) + b_4(a - a_{\mathrm{ref}})$$

$$\boxed{R_{\mathcal{O}} \equiv \frac{\mathcal{O}_{\mathrm{Ru}}}{\mathcal{O}_{\mathrm{Zr}}} \approx 1 + c_1\Delta\beta_2^2 + c_2\Delta\beta_3^2 + c_3\Delta R_0 + c_4\Delta a}$$

Species	β_2	β_3	a_0	R_0
Ru	0.162	0	0.46 fm	5.09 fm
Zr	0.06	0.20	0.52 fm	5.02 fm
difference	$\Delta\beta_2^2$	$\Delta\beta_3^2$	Δa_0	ΔR_0
	0.0226	-0.04	-0.06 fm	0.07 fm

Only probes isobar differences

2109.00131

Structure influences everywhere

$$R_{\mathcal{O}} \equiv \frac{\mathcal{O}_{\mathrm{Ru}}}{\mathcal{O}_{\mathrm{Zr}}}$$

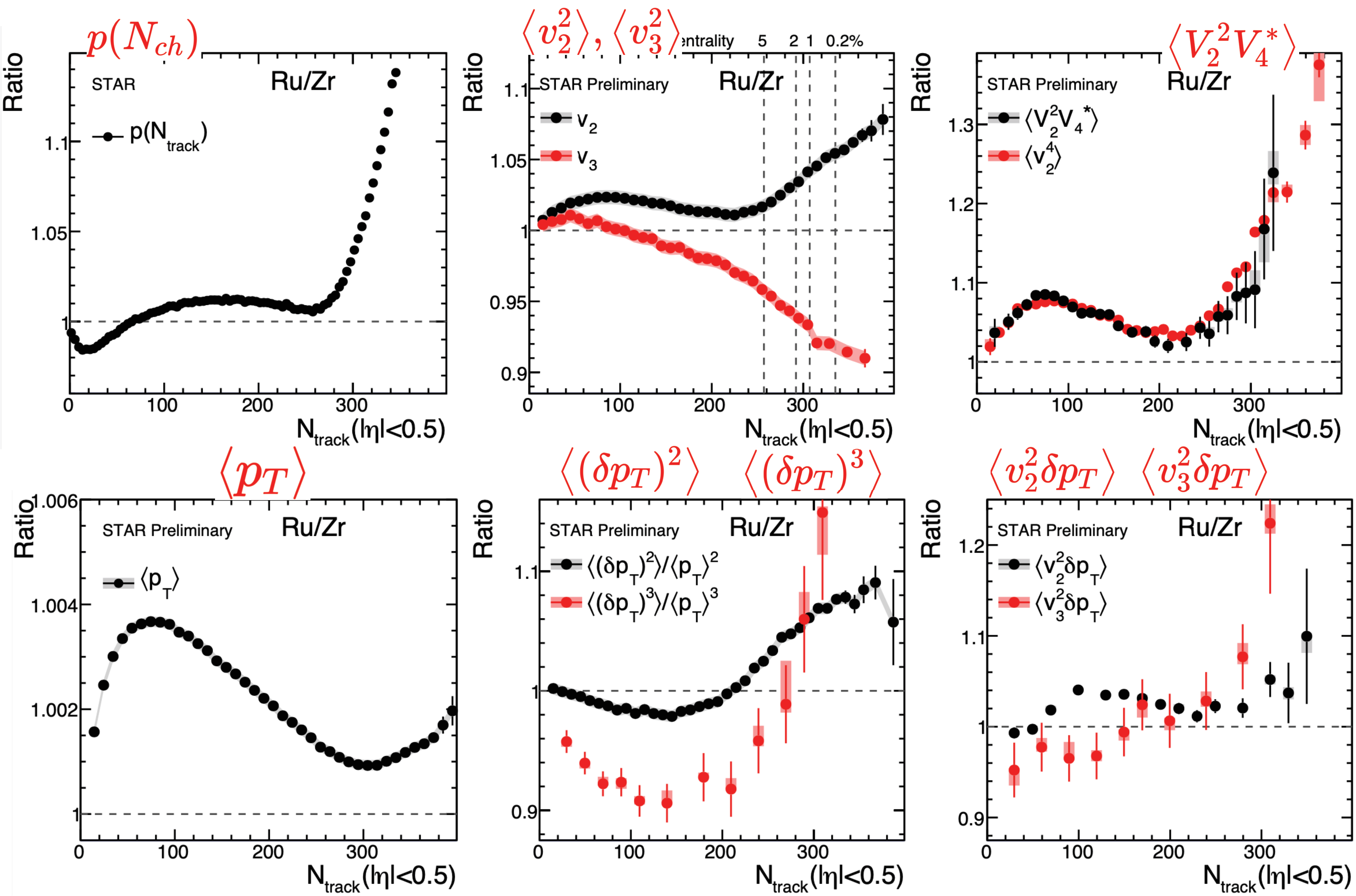

Nuclear structure via v_n-ratio

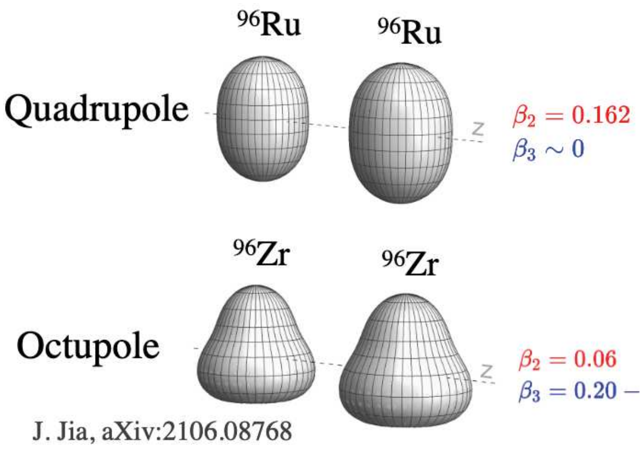

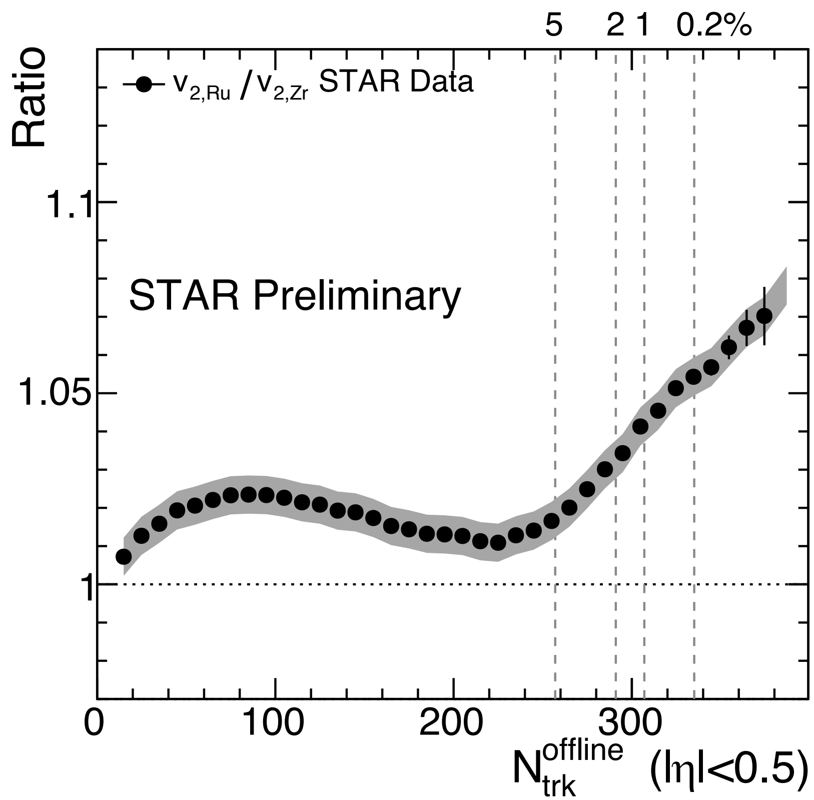

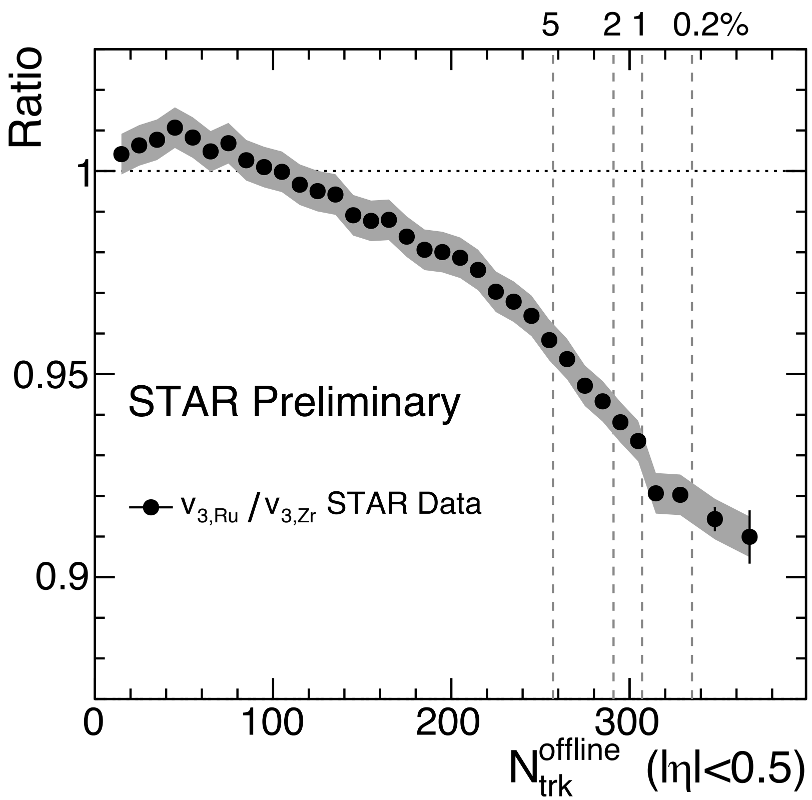

Simultaneously constrain these parameters using different N_{ch} regions

Nuclear structure via v_n-ratio

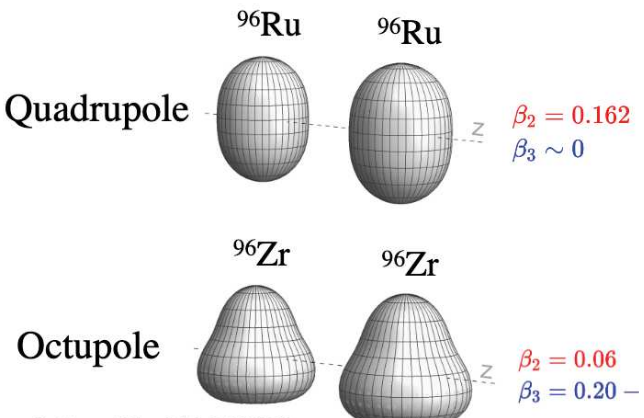

J. Jia, aXiv:2106.08768

- β_{2Ru}~0.16 increase v_2, no influence on v_3 ratio

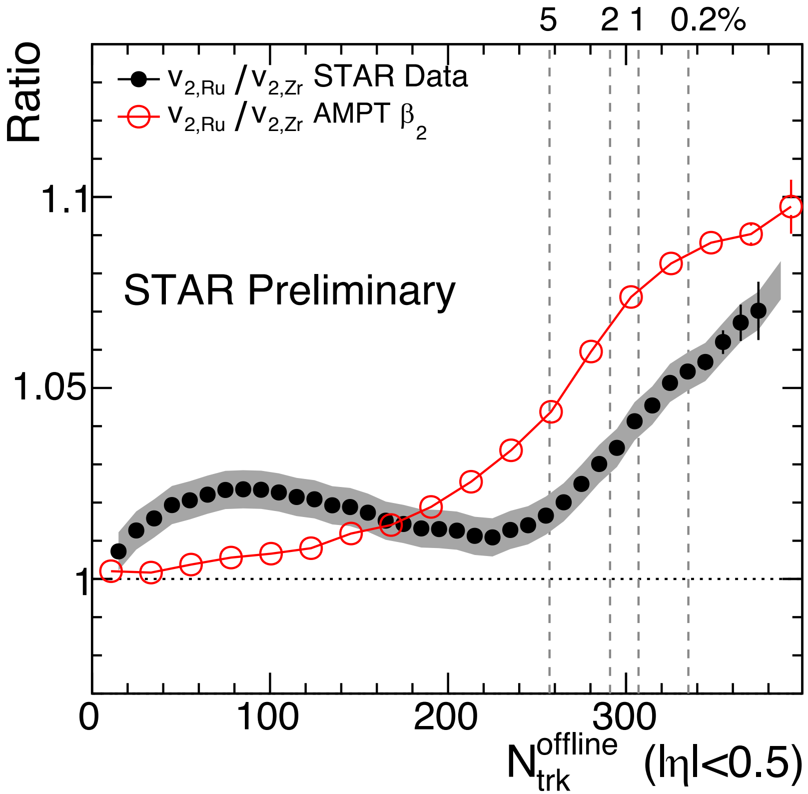

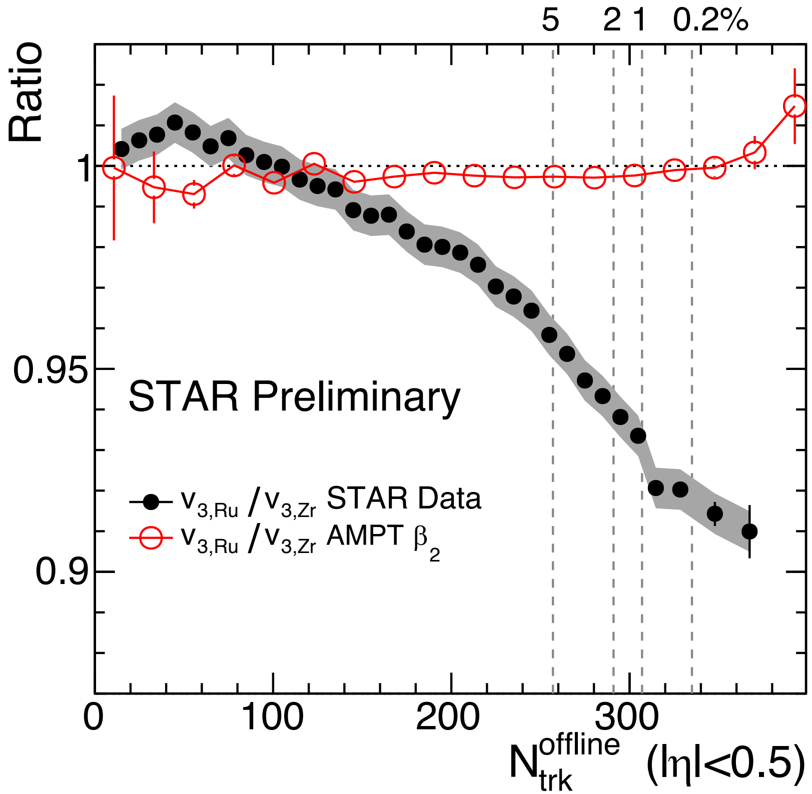

Simultaneously constrain these parameters using different N_{ch} regions

Nuclear structure via v_n-ratio

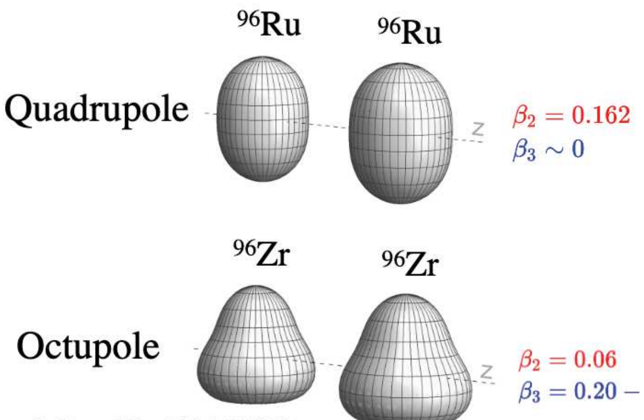

J. Jia, aXiv:2106.08768

- β_{2Ru}~0.16 increase v_2, no influence on v_3 ratio
- β_{3Zr}~0.2 decrease v_2 in mid-central, decrease v_3 ratio

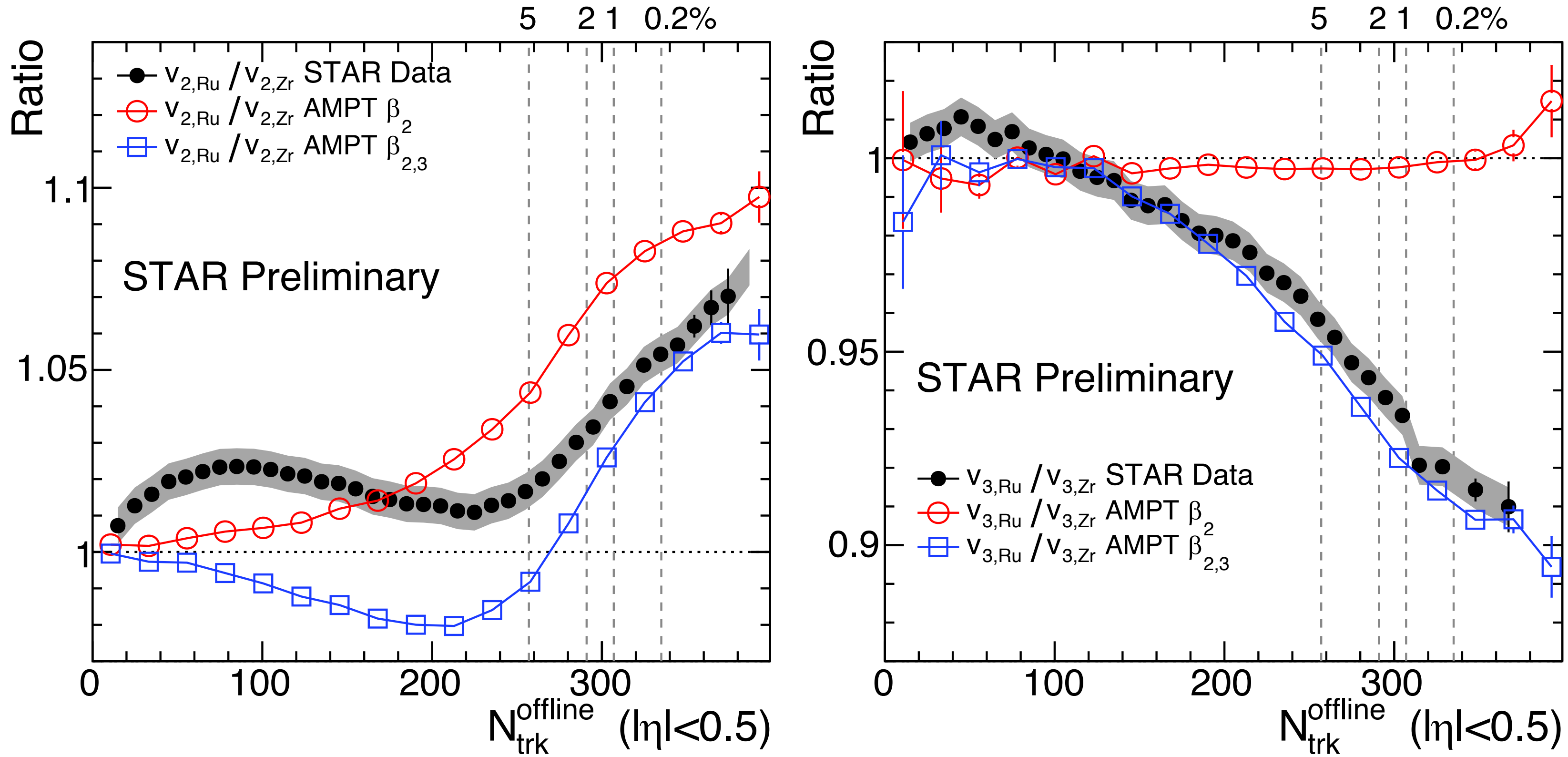

Simultaneously constrain these parameters using different N_{ch} regions

Nuclear structure via v_n-ratio

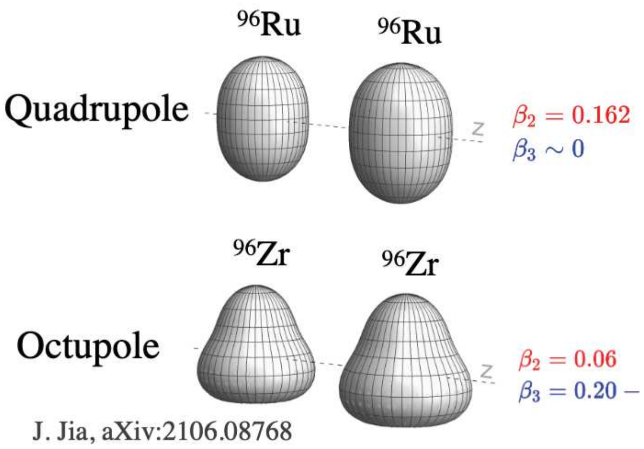

- β_{2Ru}~0.16 increase v_2, no influence on v_3 ratio
- β_{3Zr}~0.2 decrease v_2 in mid-central, decrease v_3 ratio
- Δa_0= -0.06fm increase v_2 mid-central, small influ. on v_3.

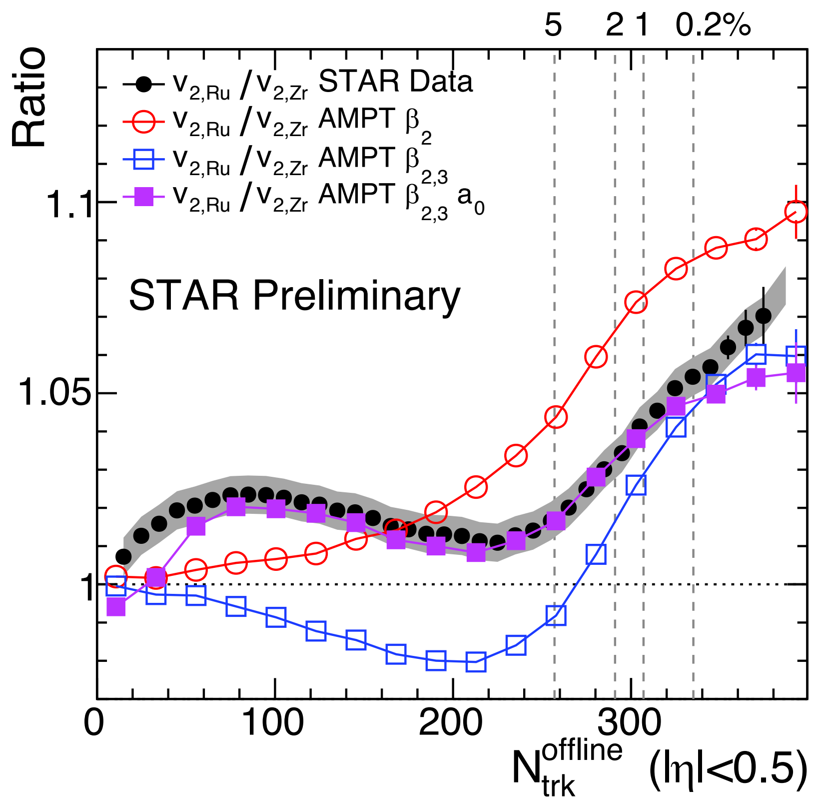

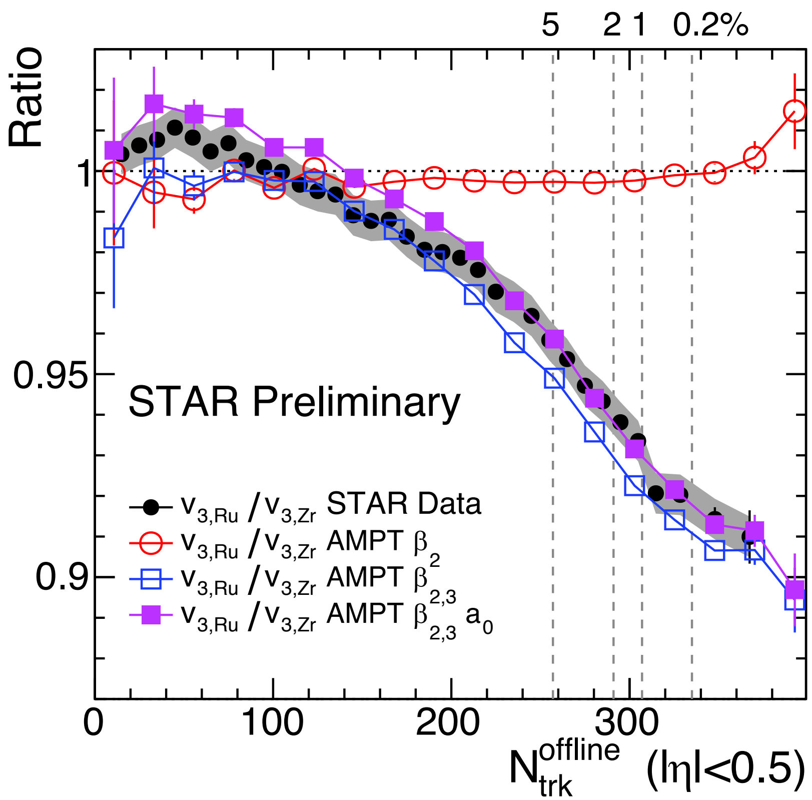

Simultaneously constrain these parameters using different N_{ch} regions

Nuclear structure via v_n-ratio

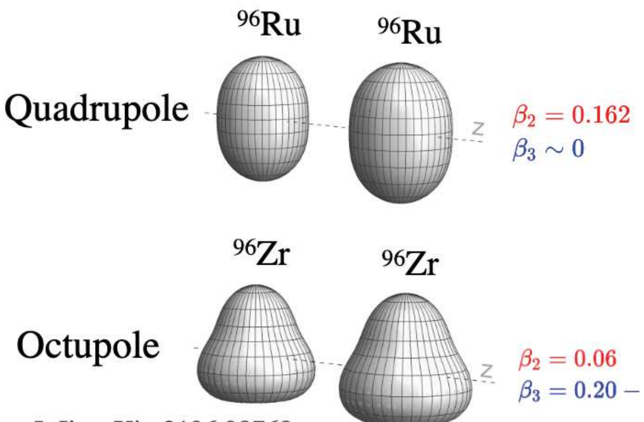

J. Jia, aXiv:2106.08768

- β_{2Ru}~0.16 increase v_2, no influence on v_3 ratio
- β_{3Zr}~0.2 decrease v_2 in mid-central, decrease v_3 ratio
- Δa_0= -0.06fm increase v_2 mid-central, small influ. on v_3.
- Radius ΔR_0=0.07fm only slightly affects v_2 and v_3 ratio.

$$R_{\mathcal{O}} \equiv \frac{\mathcal{O}_{\mathrm{Ru}}}{\mathcal{O}_{\mathrm{Zr}}} \approx 1 + c_1\Delta\beta_2^2 + c_2\Delta\beta_3^2 + c_3\Delta R_0 + c_4\Delta a$$

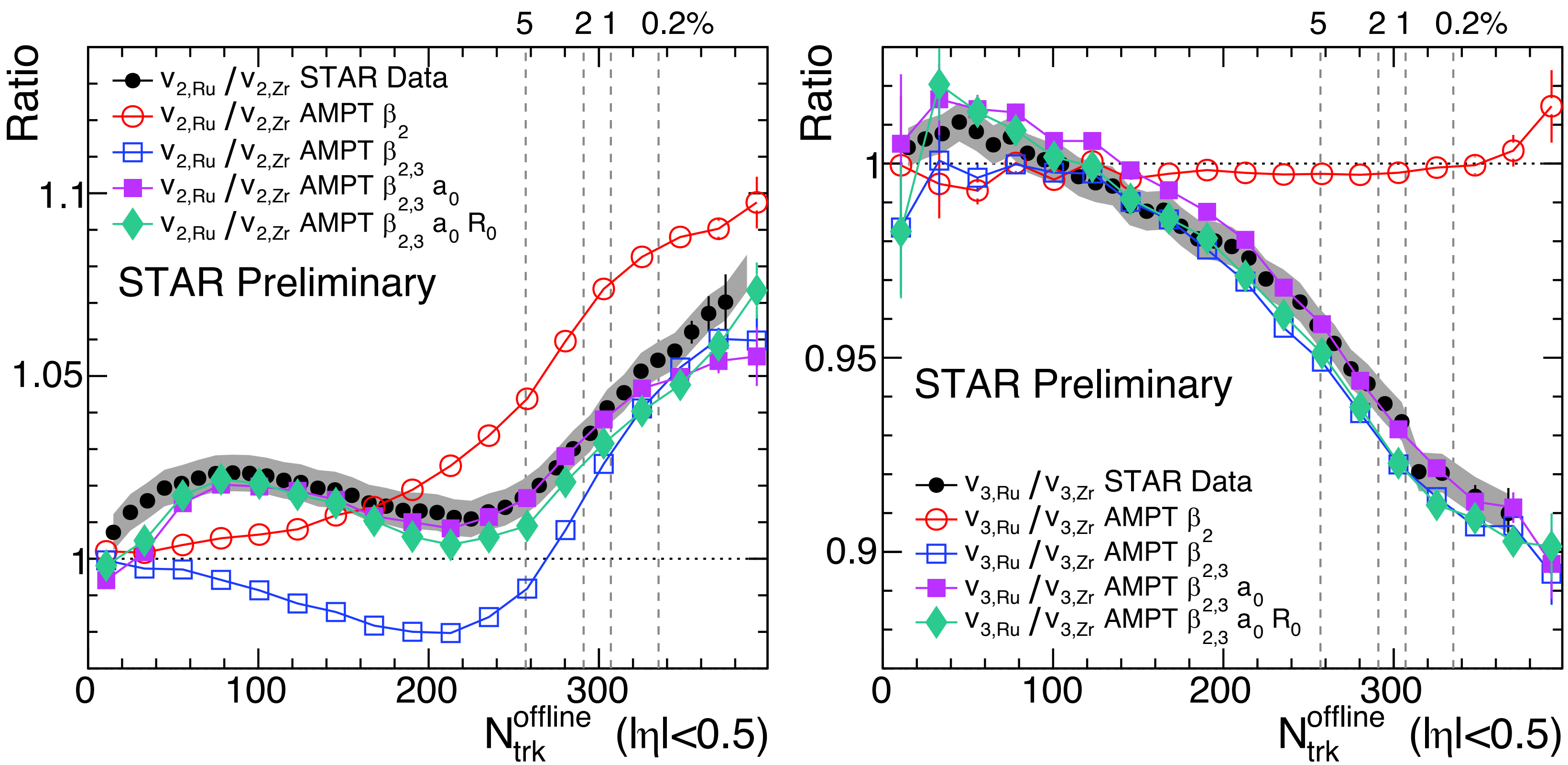

Simultaneously constrain these parameters using different N_{ch} regions

Separating shape and size effects

Nuclear skin contributes to $v_2^{rp} \sim v_2\{4\}$,
deformation contribute to fluctuations

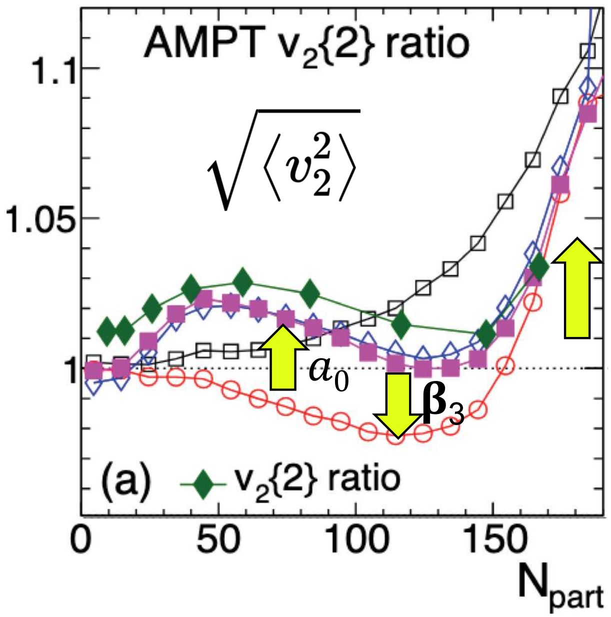

$$\langle v_2^2 \rangle = \underbrace{(v_2^{\mathrm{rp}})^2}_{\text{mean}} + \underbrace{\delta^2}_{\text{fluctuations}}$$

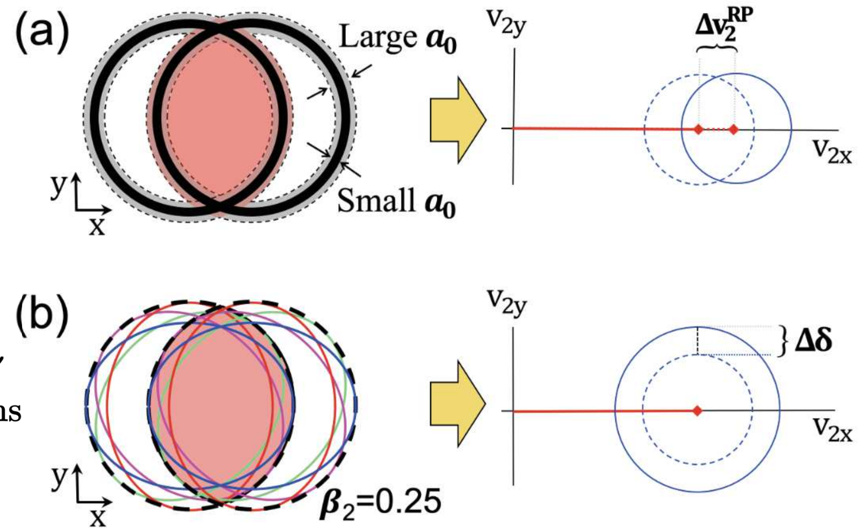

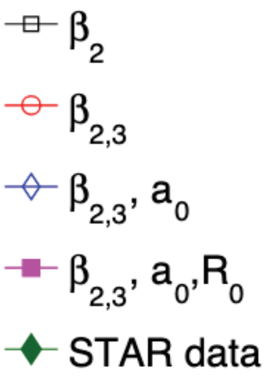

Separating shape and size effects

Nuclear skin contributes to $v_2^{rp} \sim v_2\{4\}$, deformation contribute to fluctuations

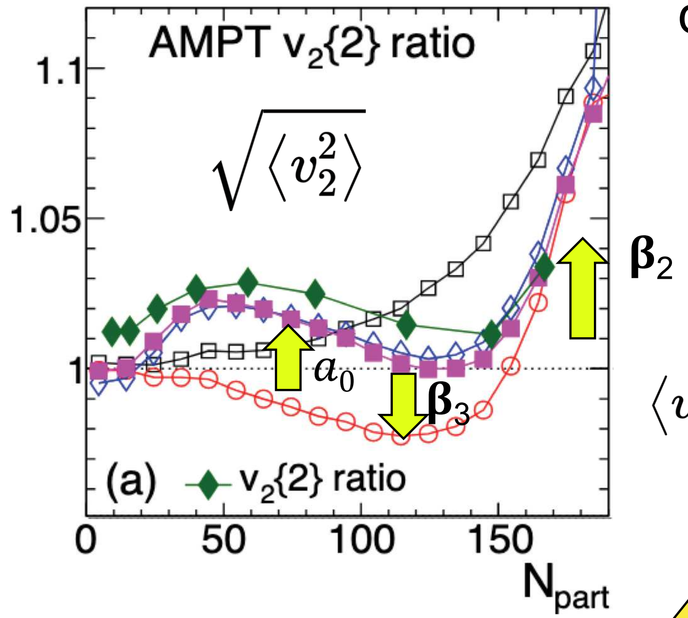

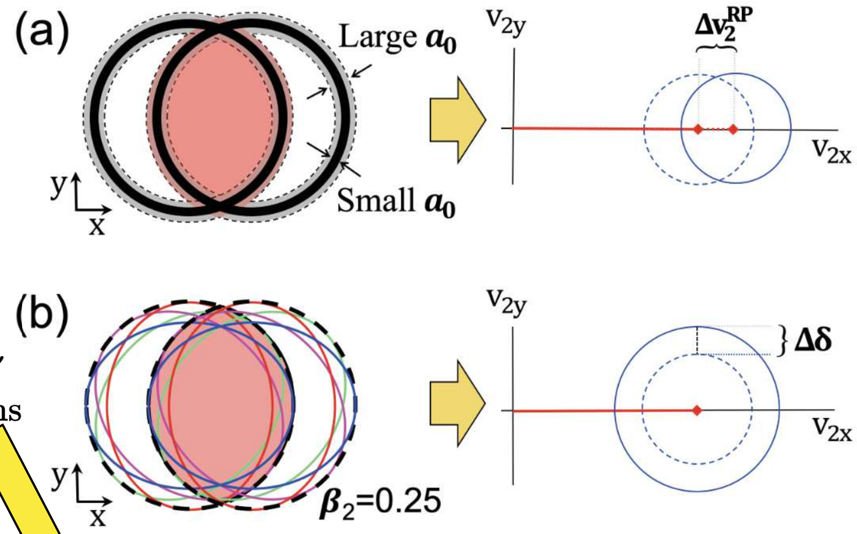

$$\langle v_2^2 \rangle = \underbrace{(v_2^{\rm rp})^2}_{\text{mean}} + \underbrace{\delta^2}_{\text{fluctuations}}$$

2206.10449

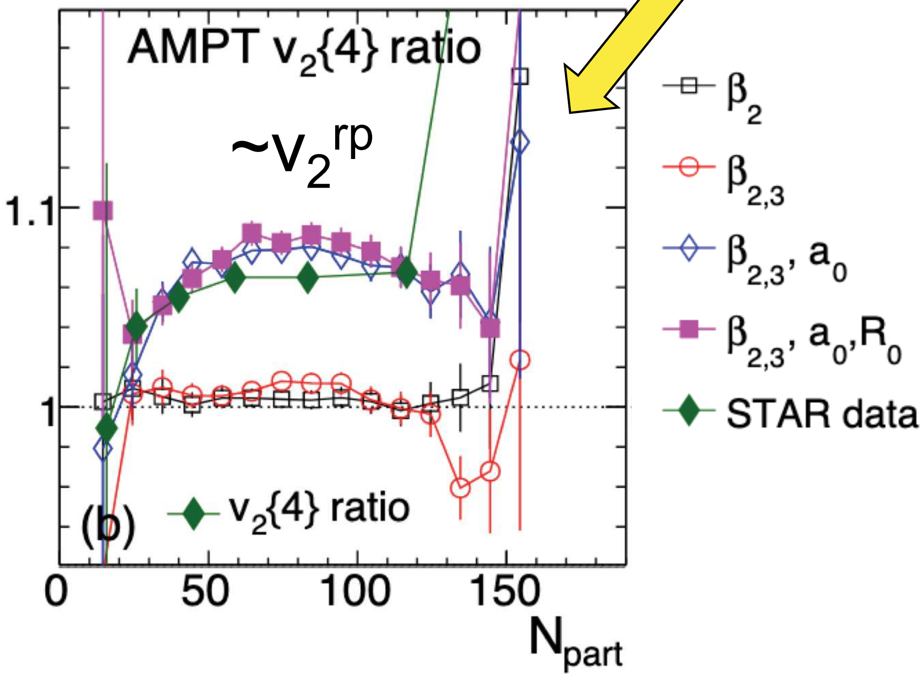

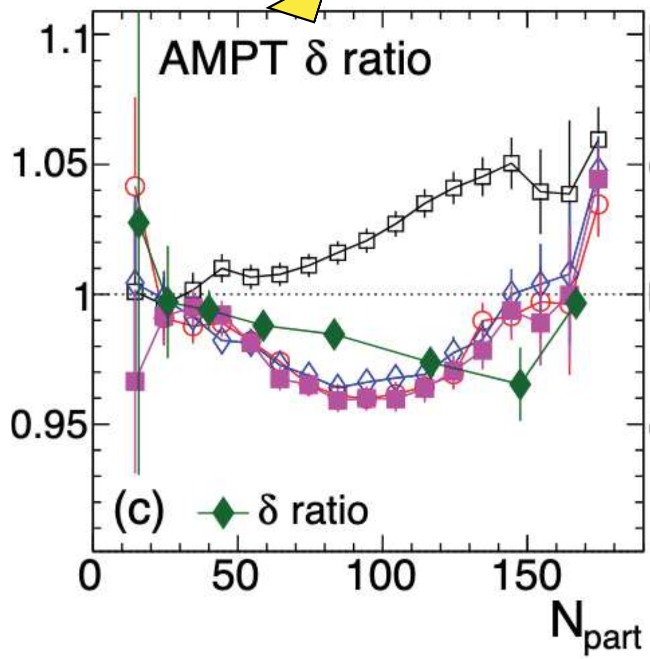

Nuclear structure via $p(N_{ch})$, <pT>-ratio

Earlier studies on this from H.Li, H.J Xu, PRL125, 222301 (2020) arXiv:2111.14812

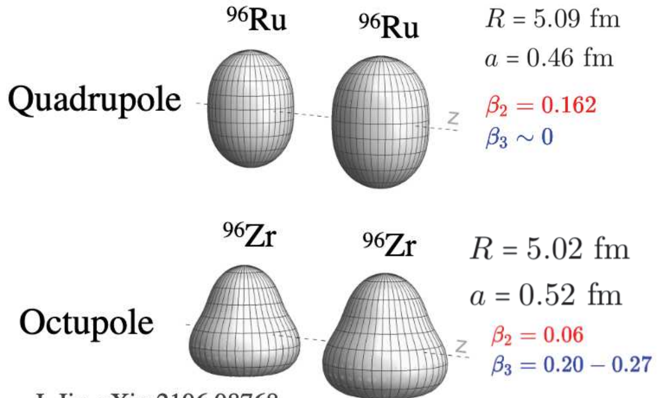

J. Jia, aXiv:2106.08768

- For Nch ratio:
  - β_{2Ru}~0.16 decrease ratio, increase after considering β_{3Zr}~0.2
  - The bump structure in non-central region from Δa_0 and ΔR_0
- For <pT> ratio:
  - Strong influence from Δa_0 and ΔR_0

$$R_{\mathcal{O}} \equiv \frac{\mathcal{O}_{\mathrm{Ru}}}{\mathcal{O}_{\mathrm{Zr}}} \approx 1 + c_1 \Delta\beta_2^2 + c_2 \Delta\beta_3^2 + c_3 \Delta R_0 + c_4 \Delta a$$

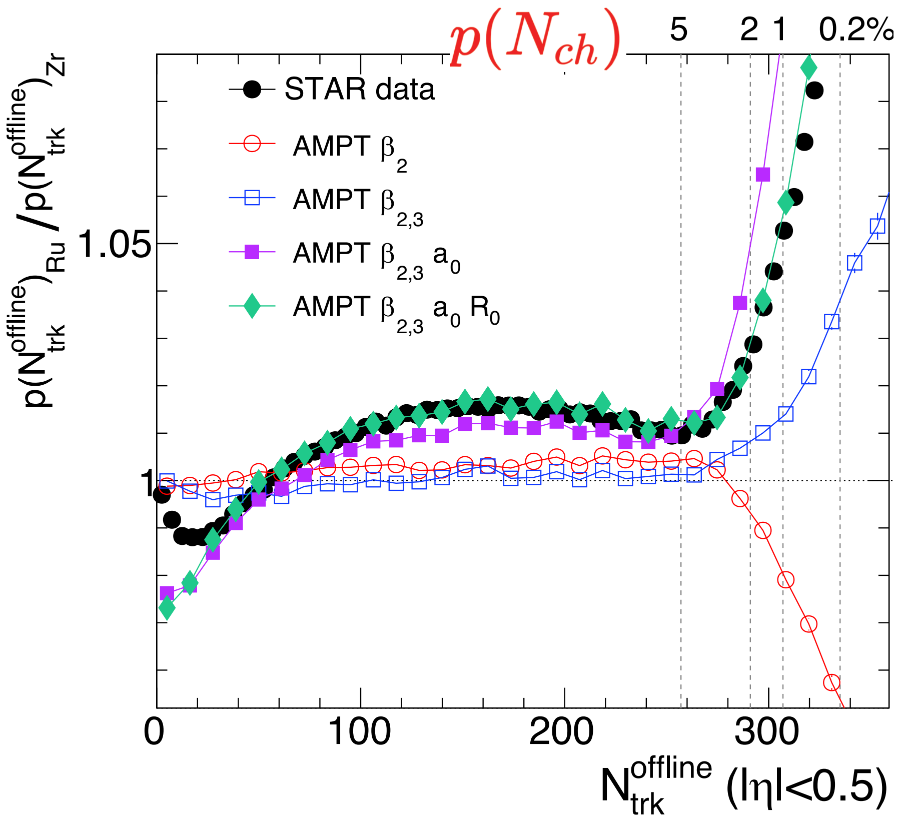

Δa_0 and ΔR_0 influences add up

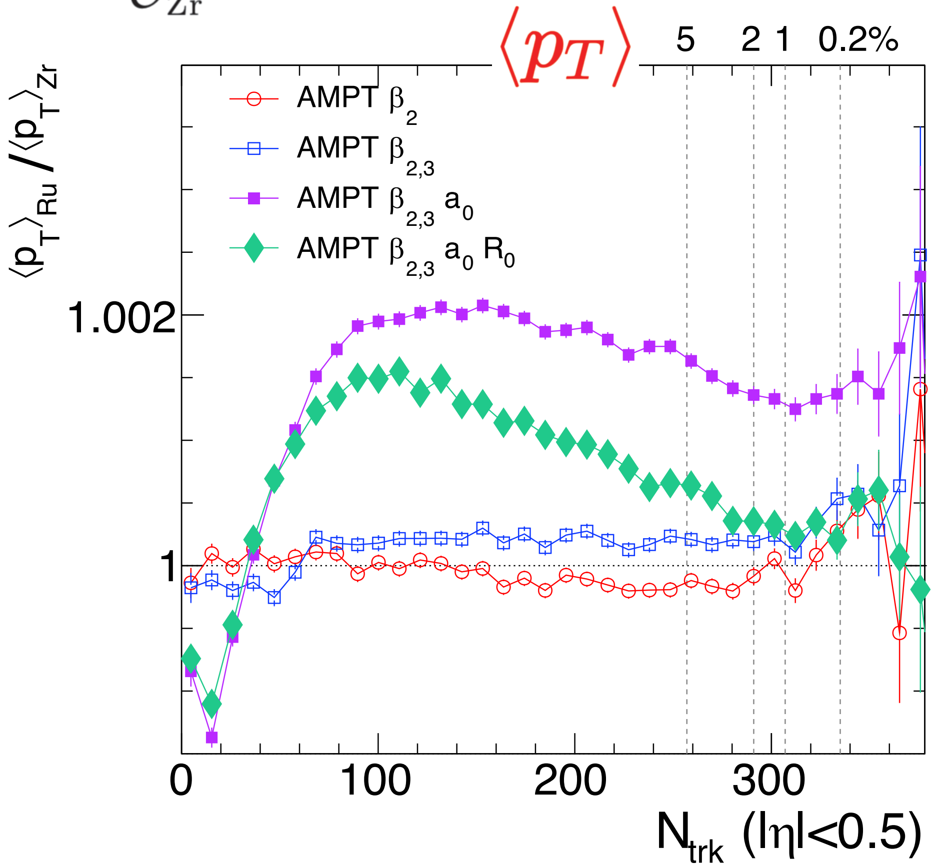

Δa_0 and ΔR_0 influences cancel

Relating to neutron skin: $\Delta r_{\mathrm{np}} = \langle r_n \rangle^{1/2} - \langle r_p \rangle^{1/2}$

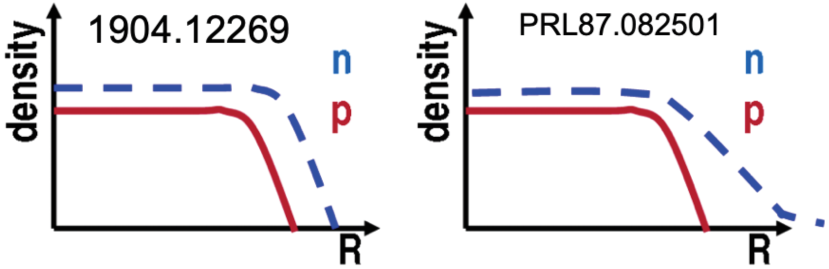

skin-type: larger R_0 halo-type: larger a_0

arXiv:2111.15559

$$\Delta r_{np} \approx \frac{\langle r^2 \rangle - \langle r_p^2 \rangle}{\sqrt{\langle r^2 \rangle}(\delta + 1)} \qquad \delta = (N - Z)/A$$

Neutron skin Δ_{np} expressed by R_0 and a_0 for nucleons and protons:

$$R_{\mathcal{O}} \equiv \frac{\mathcal{O}_{\mathrm{Ru}}}{\mathcal{O}_{\mathrm{Zr}}} \approx 1 + c_1 \Delta\beta_2^2 + c_2 \Delta\beta_3^2 + c_3 \Delta R_0 + c_4 \Delta a$$

For Woods-Saxon:

$$\langle r^2 \rangle \approx \left(\frac{3}{5} R_0^2 + \frac{7}{5} \pi^2 a^2 \right)$$

$$\langle r_p^2 \rangle \approx \left(\frac{3}{5} R_{0,p}^2 + \frac{7}{5} \pi^2 a_p^2 \right)$$

Relating to neutron skin: $\Delta r_{\mathrm{np}} = \langle r_n \rangle^{1/2} - \langle r_p \rangle^{1/2}$

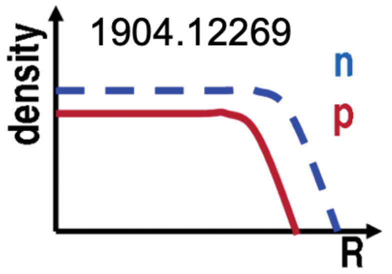

skin-type: larger R_0

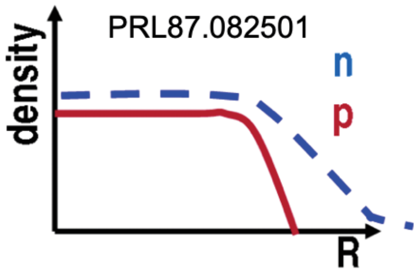

halo-type: larger a_0

arXiv:2111.15559

$$\Delta r_{np} \approx \frac{\langle r^2 \rangle - \langle r_p^2 \rangle}{\sqrt{\langle r^2 \rangle}(\delta + 1)} \qquad \delta = (N - Z)/A$$

Neutron skin Δ_{np} expressed by R_0 and a_0 for nucleons and protons:

$$R_{\mathcal{O}} \equiv \frac{\mathcal{O}_{\mathrm{Ru}}}{\mathcal{O}_{\mathrm{Zr}}} \approx 1 + c_1 \Delta\beta_2^2 + c_2 \Delta\beta_3^2 + c_3 \Delta R_0 + c_4 \Delta a$$

For Woods-Saxon:

$$\langle r^2 \rangle \approx \left(\frac{3}{5} R_0^2 + \frac{7}{5} \pi^2 a^2 \right)$$

$$\langle r_p^2 \rangle \approx \left(\frac{3}{5} R_{0,p}^2 + \frac{7}{5} \pi^2 a_p^2 \right)$$

Isobar collision measure "difference of neutron skin" from ΔR_0 Δa for nucleons, and known ΔR_0 Δa for protons:

$$\boxed{\Delta(\Delta r_{np}) = \Delta r_{np,1} - \Delta r_{np,2} \approx \frac{\Delta Y - \frac{7\pi^2}{3} \frac{\bar{a}^2}{\bar{R}_0^2} \left(\frac{\Delta Y}{2} + \bar{Y} \left(\frac{\Delta a}{\bar{a}} - \frac{\Delta R_0}{\bar{R}_0} \right) \right)}{\sqrt{15} \bar{R}_0 \left(1 + \bar{\delta} \right)}}$$

$$\Delta x = x_1 - x_2 \qquad \bar{x} = (x_1 + x_2)/2 \qquad Y \equiv 3(R_0^2 - R_{0,p}^2) + 7\pi^2 (a^2 - a_p^2)$$

Directly peeling off the skin matter

- Similar to low energy fragmentation reaction

Andrea Jedele

TECHNISCHE UNIVERSITÄT DARMSTADT NuSym2021

$$\boxed{\sigma_R} = \sigma_R^{\mathrm{NN}} + \sigma_R^{coll}$$

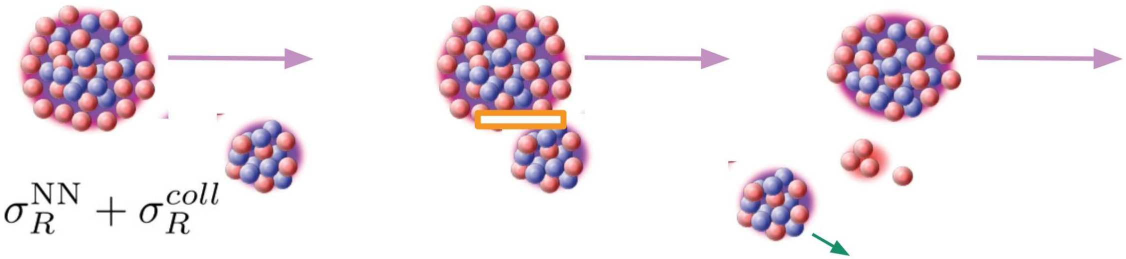

- Spectator neutrons in ultra-central isobar collisions is enhanced by neutron skin

N.Kozyrev, I. Pshenichnov 2204.07189

L. Liu, J. Xu et.al 2203.09924

Complete separation between participant and spectator matter

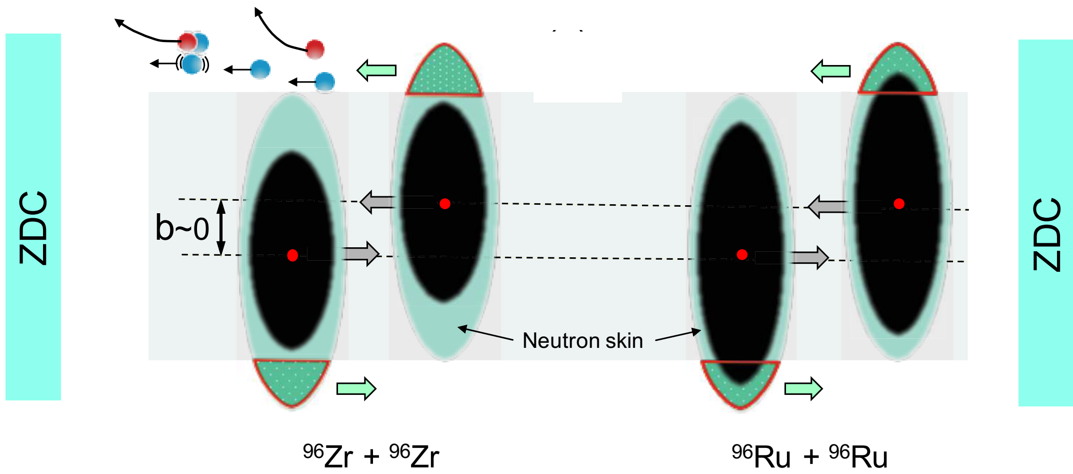

Isobar ratios not affected by final state

- Vary the shear viscosity via partonic cross-section
  - Flow signal change by 30-50%, the v_n ratio unchanged.

$$v_n = k_n \varepsilon_n$$

$$\frac{v_{n,\mathrm{Ru}}}{v_{n,\mathrm{Zr}}} \approx \frac{\varepsilon_{n,\mathrm{Ru}}}{\varepsilon_{n,\mathrm{Zr}}}$$

Robust probe of initial state!

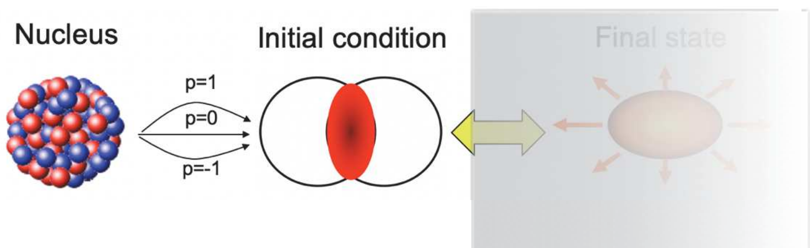

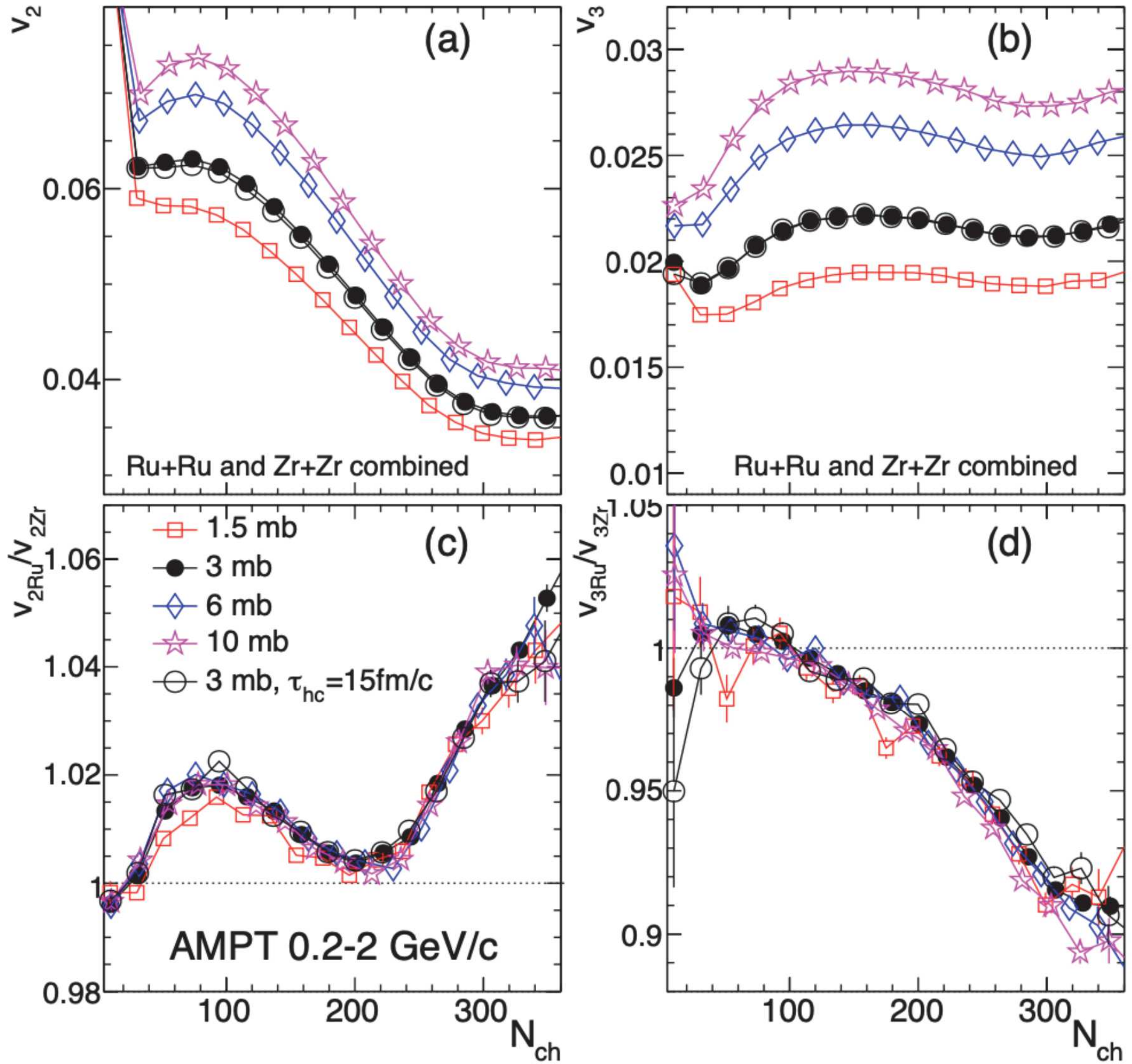

Isobar to constrain initial condition

Nucleus Initial condition Final state

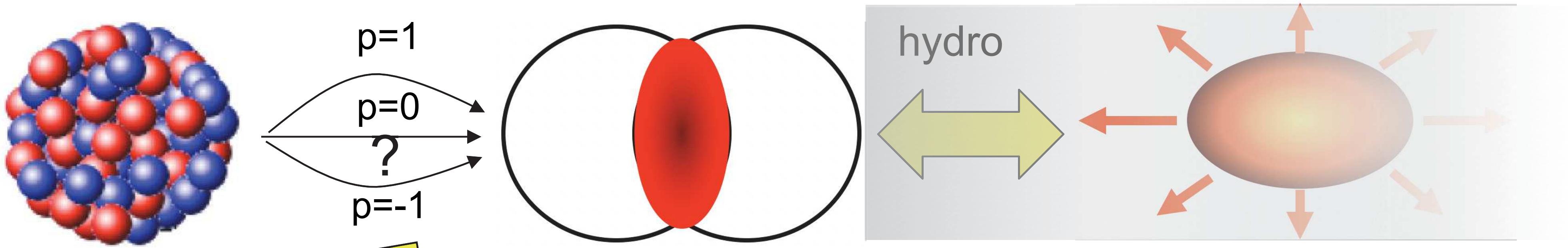

$$T_A(x,y) = \int \rho(x,y,z)dz$$

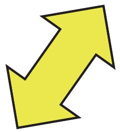

$$\frac{\mathcal{O}_{\mathrm{Ru}}}{\mathcal{O}_{\mathrm{Zr}}} \approx 1 + c_1\Delta\beta_2^2 + c_2\Delta\beta_3^2 + c_3\Delta R_0 + c_4\Delta a$$

c_n relates nuclear structure and initial condition

- Different ways of depositing energy $T \propto \left(\frac{T_A^p + T_B^p}{2}\right)^{q/p}$

$$e(x,y) \sim \begin{cases} T_A + T_B & N_{\text{part}} - \text{scaling}, p = 1 \\ T_A T_B & N_{\text{coll}} - \text{scaling}, p = 0, q = 2 \\ \sqrt{T_A T_B} & \text{Trento default}, p = 0 \\ \min\{T_A, T_B\} & \text{KLN model}, p \sim -2/3 \\ T_A + T_B + \alpha T_A T_B & \text{two-component model,} \\ & \text{similar to quark-glauber model} \end{cases}$$

Use nuclear structure as extra lever-arm for initial condition

Low-energy vs high-energy HI method

- Shape from B(En), radial profile from e+A or ion-A scattering

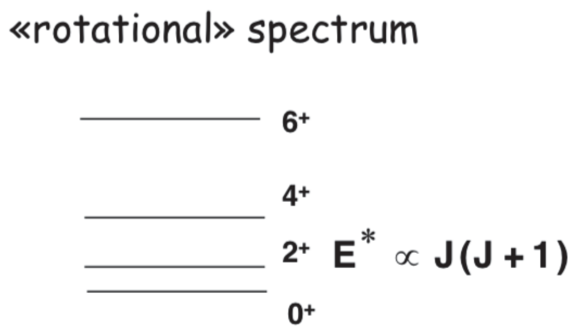

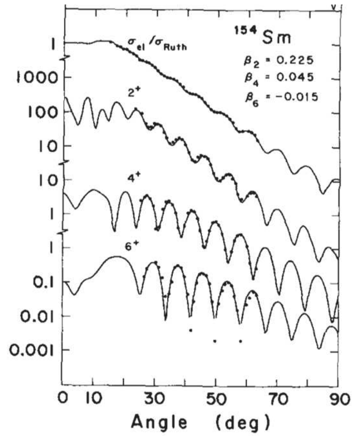

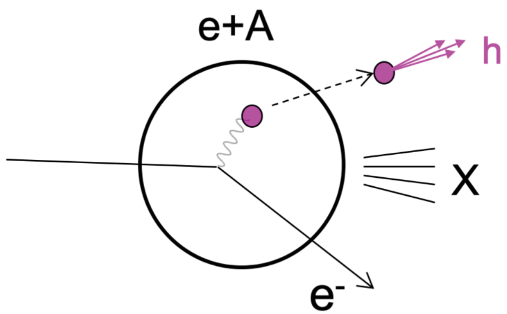

- Shape frozen in crossing time ($<10^{-24}$s), probe entire mass distribution via multi-point correlations.

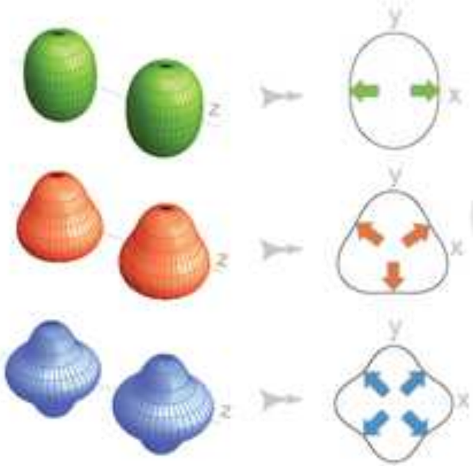

Collective flow response to nuclear structure

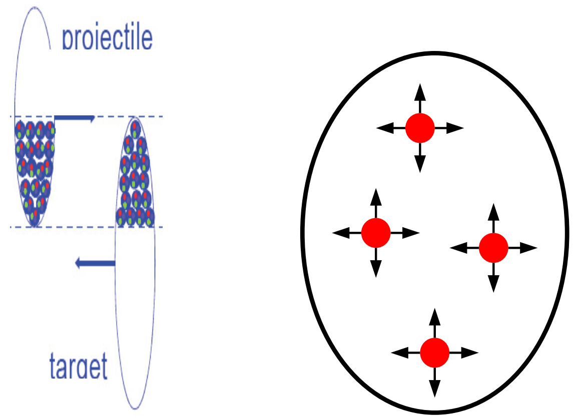

$$S(\mathbf{s}_1,\mathbf{s}_2) \equiv \langle \delta\rho(\mathbf{s}_1)\delta\rho(\mathbf{s}_2)\rangle$$
$$= \langle \rho(\mathbf{s}_1)\rho(\mathbf{s}_2)\rangle - \langle \rho(\mathbf{s}_1)\rangle\langle \rho(\mathbf{s}_2)\rangle.$$

higher-order correlations

- In principle, can measure any moments of p(1/R, ε_2, ε_3…)
  - Mean $\langle d_\perp \rangle$ $\quad\quad$ $\langle p_T \rangle$
  - Variances: $\langle \varepsilon_n^2 \rangle$, $\left\langle (\delta d_\perp / d_\perp)^2 \right\rangle$ $\quad d_\perp \equiv 1/R_\perp$ $\quad\quad$ $\langle v_n^2 \rangle$, $\left\langle (\delta p_T / p_T)^2 \right\rangle$
  - Skewness $\langle \varepsilon_n^2 \delta d_\perp / d_\perp \rangle$, $\left\langle (\delta d_\perp / d_\perp)^3 \right\rangle$ $\quad\quad$ $\langle v_n^2 \delta p_T / p_T \rangle$, $\left\langle (\delta p_T / p_T)^3 \right\rangle$
  - Kurtosis $\langle \varepsilon_n^4 \rangle - 2\langle \varepsilon_n^2 \rangle^2$, $\left\langle (\delta d_\perp / d_\perp)^4 \right\rangle - 3\left\langle (\delta d_\perp / d_\perp)^2 \right\rangle^2$ $\quad$ $\langle v_n^4 \rangle - 2\langle v_n^2 \rangle^2$, $\left\langle (\delta p_T / p_T)^4 \right\rangle - 3\left\langle (\delta p_T / p_T)^2 \right\rangle^2$

    …
- All with rather simple expressions, for example:
  - Skewness

$$\left\langle \varepsilon_2^2 \delta d_\perp / d_\perp \right\rangle \sim a_1 - b_1 \cos(3\gamma)\beta_2^3$$

$$\left\langle (\delta d_\perp / d_\perp)^3 \right\rangle \sim a_2 + b_2 \cos(3\gamma)\beta_2^3$$

  - Kurtosis

$$\left\langle \varepsilon_2^4 \right\rangle - 2\left\langle \varepsilon_2^2 \right\rangle^2 \sim a_3 - b_3 \beta_2^4$$

$$\left\langle (\delta d_\perp / d_\perp)^4 \right\rangle - 3\left\langle (\delta d_\perp / d_\perp)^2 \right\rangle^2 \sim a_4 - b_4 \beta_2^4$$

Liquid-drop model estimate in head-on collisions

1811.03959, 2109.00604

Estimate with liquid drop model →
Nucleus with a sharp surface: $\rho(r,\theta,\phi) = \begin{cases} 1 & r < R(\theta,\phi) \\ 0 & r > R(\theta,\phi) \end{cases}$

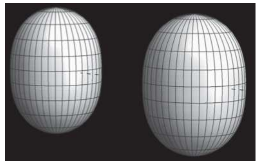

UCC collisions and ignoring nucleon fluctuations→

$$\frac{\delta d_\perp}{d_\perp} = \sqrt{\frac{5}{16\pi}}\beta_2\left(\cos\gamma D^2_{0,0} + \frac{\sin\gamma}{\sqrt{2}}\left[D^2_{0,2}+D^2_{0,-2}\right]\right), \quad \epsilon_2 = -\sqrt{\frac{15}{2\pi}}\beta_2\left(\cos\gamma D^2_{2,0} + \frac{\sin\gamma}{\sqrt{2}}\left[D^2_{2,2}+D^2_{2,-2}\right]\right)$$

$$\left\langle \varepsilon_2^2 \right\rangle = \frac{3}{4\pi}\beta_2^2 \qquad \left\langle (\delta d_\perp/d_\perp)^2 \right\rangle = \frac{1}{32\pi}\beta_2^2$$

$\left\langle (\delta d_\perp/d_\perp)^3 \right\rangle$	$\left\langle \varepsilon_2^2 (\delta d_\perp/d_\perp) \right\rangle$	$\left\langle \varepsilon_2^2 (\delta d_\perp/d_\perp)^2 \right\rangle - \left\langle \varepsilon_2^2 \right\rangle \left\langle (\delta d_\perp/d_\perp)^2 \right\rangle$
$\frac{\sqrt{5}}{896\pi^{3/2}}\cos(3\gamma)\beta_2^3$	$-\frac{3\sqrt{5}}{112\pi^{3/2}}\cos(3\gamma)\beta_2^3$	$-\frac{3}{896\pi^2}\beta_2^4$
$\left\langle (\delta d_\perp/d_\perp)^4 \right\rangle - 3\left\langle (\delta d_\perp/d_\perp)^2 \right\rangle^2$	$\left\langle \varepsilon_2^4 \right\rangle - 2\left\langle \varepsilon_2^2 \right\rangle^2$	$\left(\left\langle \varepsilon_2^6 \right\rangle - 9\left\langle \varepsilon_2^4 \right\rangle \left\langle \varepsilon_2^2 \right\rangle + 12\left\langle \varepsilon_2^2 \right\rangle^3\right)/4$
$-\frac{3}{7168\pi^2}\beta_2^4$	$-\frac{9}{56\pi^2}\beta_2^4$	$\frac{27(373-25\cos(6\gamma))}{32\times 8008\pi^3}\beta_2^6$

Triaxility

$$R(\theta,\phi) = R_0\left(1 + \beta_2[\cos\gamma Y_{2,0} + \sin\gamma Y_{2,2}]\right.$$

1910.04673, 2004.14463

Prolate

$\beta_2 = 0.25, \cos(3\gamma) = 1$

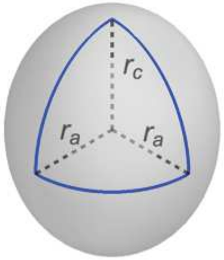

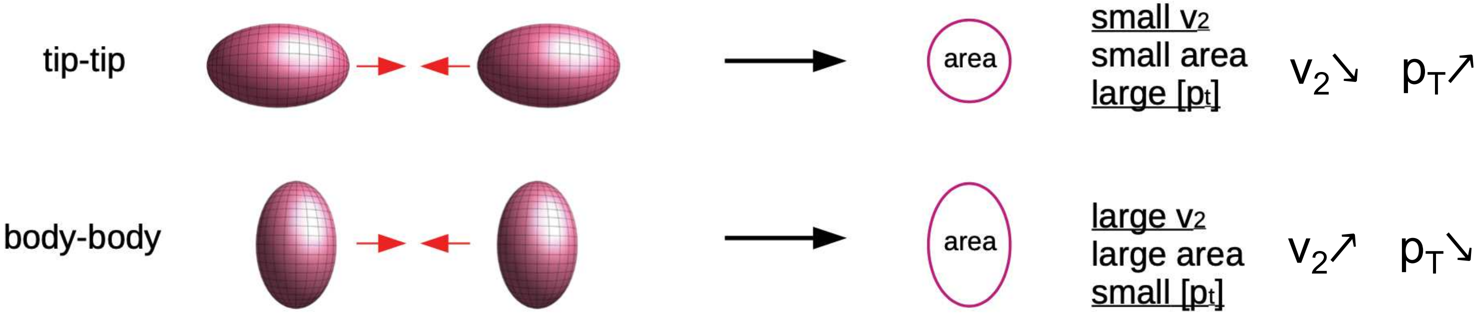

Need 3-point correlators to probe the 3 axes

$$\langle v_2^2 \delta p_\mathrm{T} \rangle \sim -\beta_2^3 \cos(3\gamma) \qquad \langle (\delta p_\mathrm{T})^3 \rangle \sim \beta_2^3 \cos(3\gamma)$$

2109.00604

Triaxial

$\beta_2 = 0.25, \cos(3\gamma) = 0$

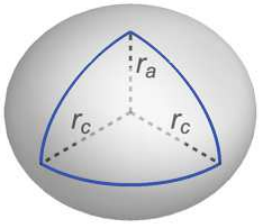

Oblate

$\beta_2 = 0.25, \cos(3\gamma) = -1$

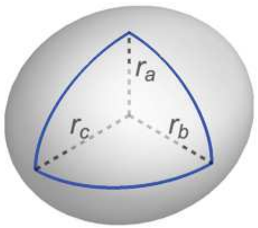

Triaxility $R(\theta,\phi) = R_0\left(1 + \beta_2[\cos\gamma Y_{2,0} + \sin\gamma Y_{2,2}]\right.$

1910.04673, 2004.14463

Prolate

$\beta_2 = 0.25, \cos(3\gamma) = 1$

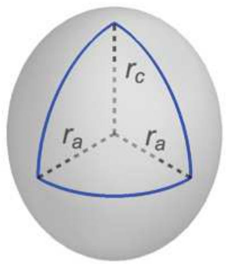

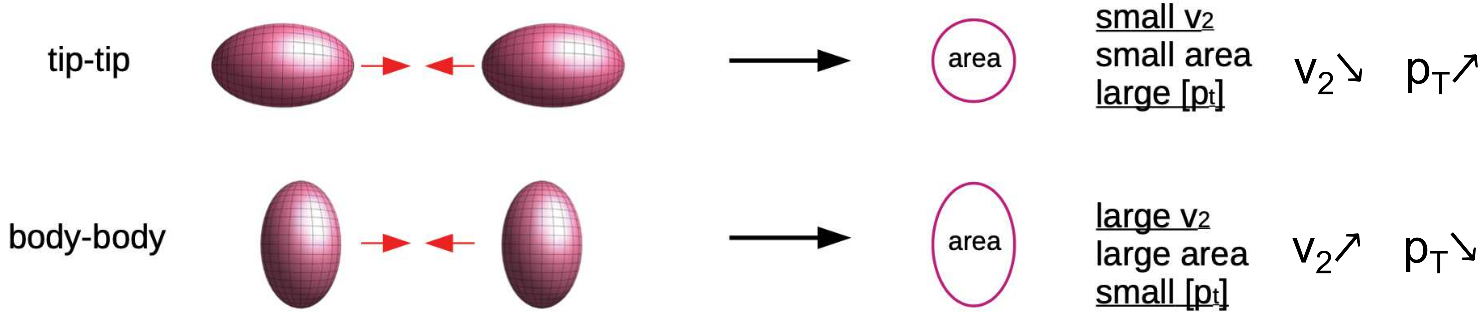

Need 3-point correlators to probe the 3 axes

$$\left\langle v_2^2 \delta p_T \right\rangle \sim -\beta_2^3 \cos(3\gamma) \qquad \left\langle (\delta p_T)^3 \right\rangle \sim \beta_2^3 \cos(3\gamma)$$

2109.00604

Triaxial

$\beta_2 = 0.25, \cos(3\gamma) = 0$

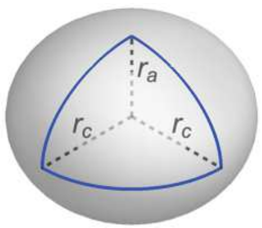

Compare U+U vs Au+Au: β_{2U} ~ 0.28, β_{2Au}~ 0.13:

Oblate

$\beta_2 = 0.25, \cos(3\gamma) = -1$

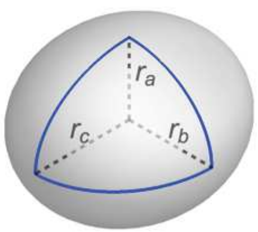

v_2-[p_T] covariance

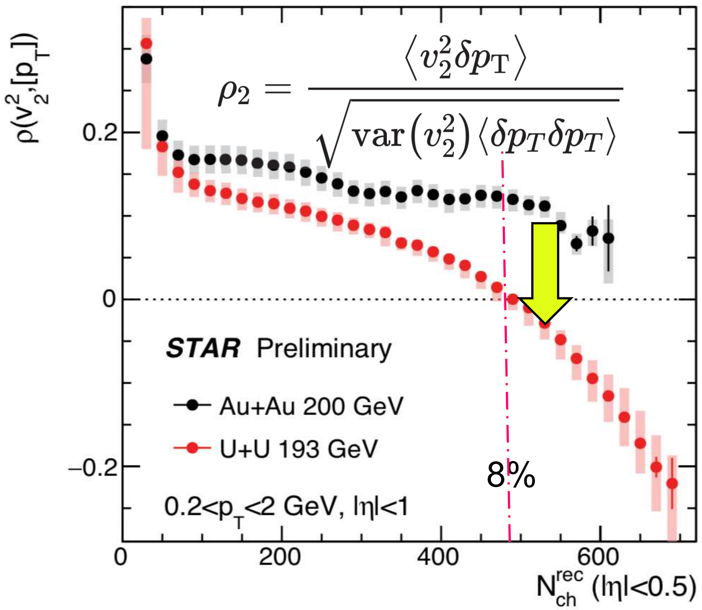

[p_T] skewness

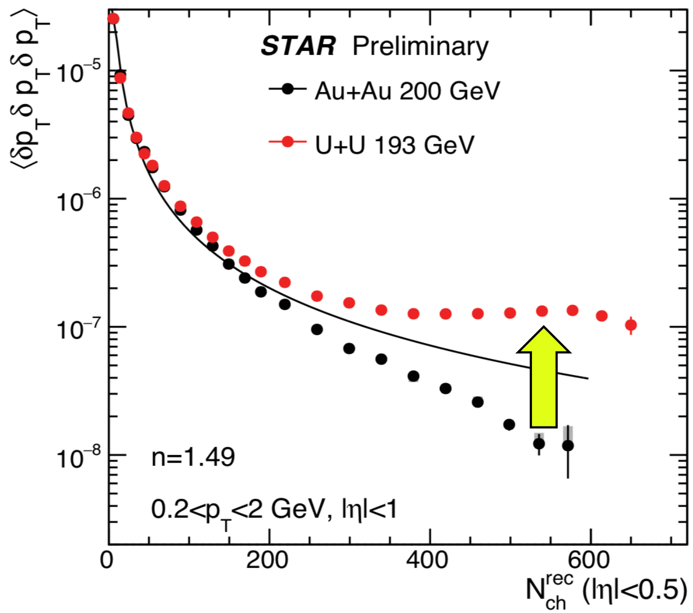

Influence of triaxiality: Glauber model

Skewness super sensitive

Described by

$$\left\langle \varepsilon_2^2 \frac{\delta d_\perp}{d_\perp} \right\rangle \propto \langle v_2^2 \delta p_{\mathrm{T}} \rangle \propto a + b\cos(3\gamma)\beta_2^3$$

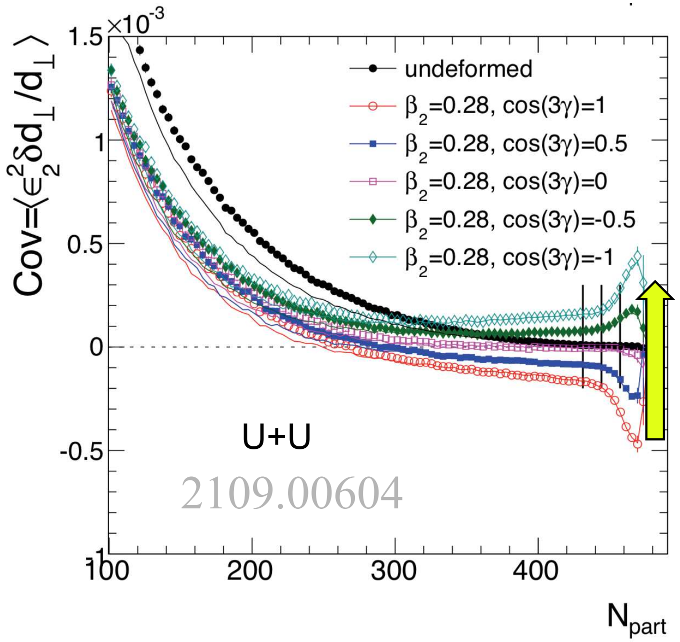

variances insensitive to γ

$$\left\langle \varepsilon_2^2 \right\rangle \propto \left\langle v_2^2 \right\rangle \propto a + b\beta_2^2$$

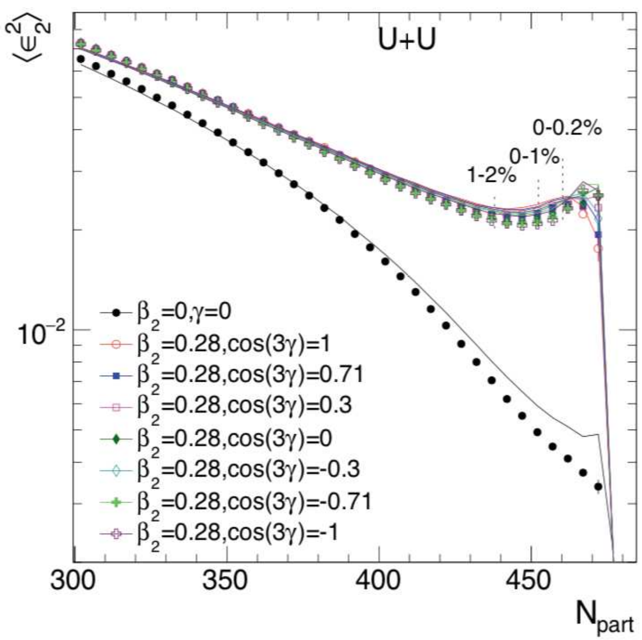

Use variance to constrain β_2, use skewness to constrain γ

(β_2,γ) diagram in heavy-ion collisions

The (β_2,γ) dependence in 0-1% U+U Glauber model can be approximated by:

$$d_\perp \propto 1/R_\perp$$

$$\langle \varepsilon_2^2 \rangle \approx [0.02 + \beta_2^2] \times 0.235$$

$$\langle (\delta d_\perp/d_\perp)^2 \rangle \approx [0.035 + \beta_2^2] \times 0.0093$$

$$\langle \varepsilon_2^2 \delta d_\perp/d_\perp \rangle \approx [0.0005 - (0.07 + 1.36\cos(3\gamma))\beta_2^3] \times 10^{-2}$$

$$\rho = \frac{\langle \varepsilon_2^2 \delta d_\perp \rangle}{\langle \varepsilon_2^2 \rangle \sqrt{\langle (\delta d_\perp)^2 \rangle}}$$

Map from (β_2,γ) plane to HI observables

How about $\langle v_2^2 \delta[p_T] \rangle$ vs. $\langle v_2^2 \rangle$

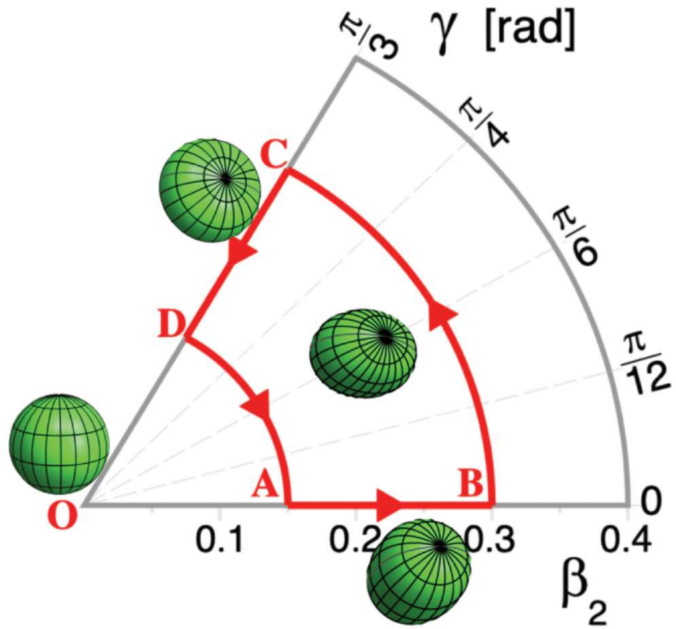

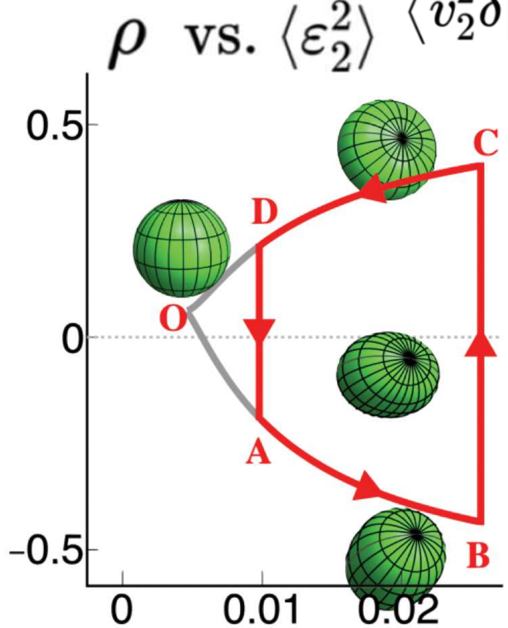

Collision system scan to map out this trajectory: calibrate coefficients with species with known β,γ, then predict for species of interest.

What future collisions can bring?

Future well-motivated system-scan to use heavy-ion collisions into a precision tool for both nuclear structure and initial condition, and ultimately improve the study of QGP.

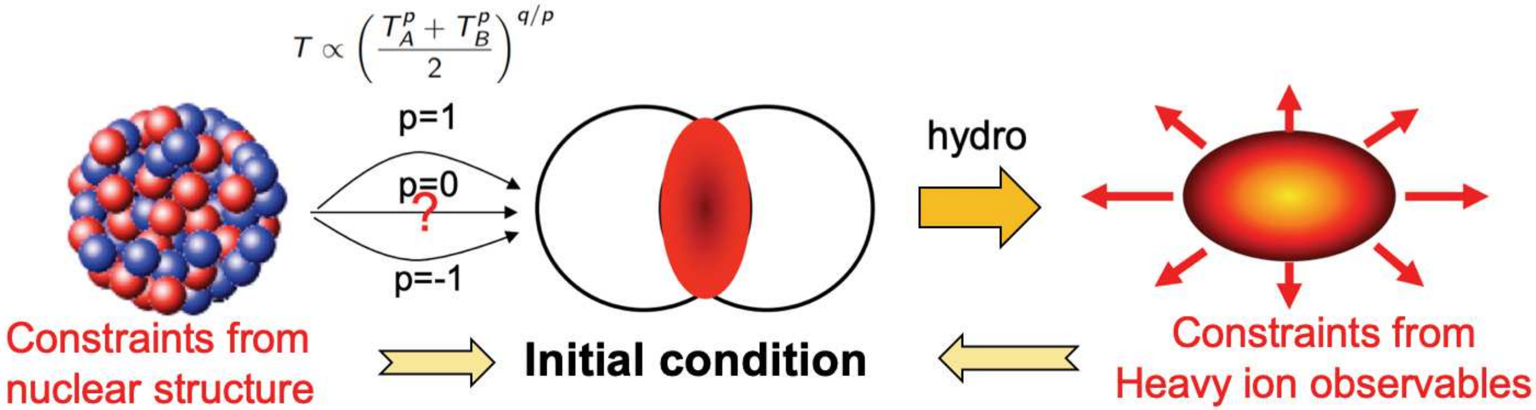

More than 250 stable (long-lived nuclei), about 140 of them in isobar pairs or triplets

A	isobars	A	isobars	A	isobars	A	isobars	A	isobars	A	isobars
36	Ar, S	80	Se, Kr	106	Pd, Cd	124	Sn, Te, Xe	148	Nd, Sm	174	Yb, Hf
40	Ca, Ar	84	Kr, Sr, Mo	108	Pd, Cd	126	Te, Xe	150	Nd, Sm	176	Yb, Lu, Hf
46	Ca, Ti	86	Kr, Sr	110	Pd, Cd	128	Te, Xe	152	Sm, Gd	180	Hf, W
48	Ca, Ti	87	Rb, Sr	112	Cd, Sn	130	Te, Xe, Ba	154	Sm, Gd	184	W, Os
50	Ti, V, Cr	92	Zr, Nb, Mo	113	Cd, In	132	Xe, Ba	156	Gd,Dy	186	W, Os
54	Cr, Fe	94	Zr, Mo	114	Cd, Sn	134	Xe, Ba	158	Gd,Dy	187	Re, Os
64	Ni, Zn	96	Zr, Mo, Ru	115	In, Sn	136	Xe, Ba, Ce	160	Gd,Dy	190	Os, Pt
70	Zn, Ge	98	Mo, Ru	116	Cd, Sn	138	Ba, La, Ce	162	Dy,Er	192	Os, Pt
74	Ge, Se	100	Mo, Ru	120	Sn, Te	142	Ce, Nd	164	Dy,Er	196	Pt, Hg
76	Ge, Se	102	Ru, Pd	122	Sn, Te	144	Nd, Sm	168	Er,Yb	198	Pt, Hg
78	Se, Kr	104	Ru, Pd	123	Sb, Te	146	Nd, Sm	170	Er,Yb	204	Hg, Pb

What future collisions can bring?

Future well-motivated system-scan to use heavy-ion collisions into a precision tool for both nuclear structure and initial condition, and ultimately improve the study of QGP.

Representative cases were identified in a dedicated EMMI taskforce among HI and structure experts.

https://indico.gsi.de/event/14430/contributions/64193/

The discussion lead to the identification of three science cases that may readily lead to breakthrough observations via relativistic collision experiments. They involve nuclides belonging, respectively, to the mass regions $A \sim 20$, $A \sim 40$, and $A \sim 150$.

A~200

Stress test small system collectivity with extreme deformability

Imaging strong shape evolution of $^{144-154}$Sm isotopic chain

Inferring the neutron skin by comparing ^{40}Ca and ^{48}Ca

Cross-calibrate the initial condition of Pb+Pb and Au+Au collisions

Stress-testing small system collectivity with 20Ne

Geometric origin of small system program is rather qualitative.

Very subtle effects if one only have 16O+16O collisions

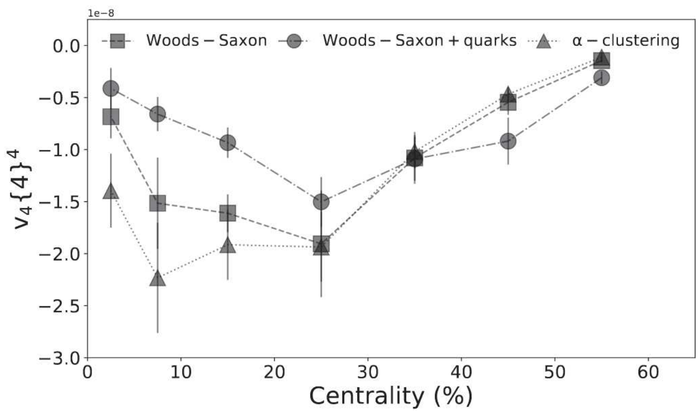

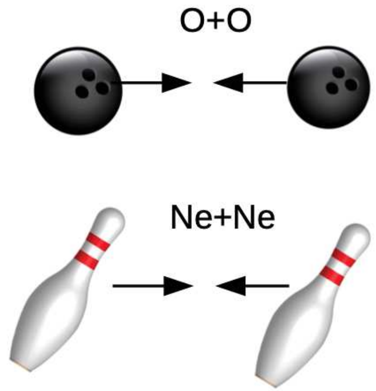

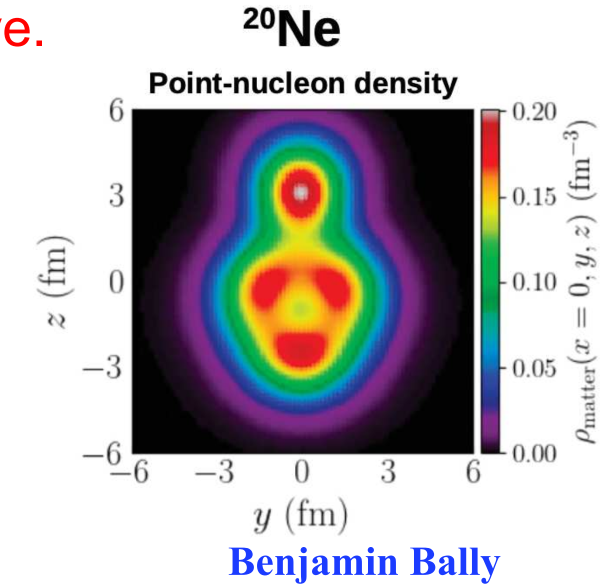

20Ne with 5 alpha has the most extreme ground state shape: $\beta_2 \sim 0.7, \beta_3 \sim 0.5$. Use O+O and Ne+Ne to observe "strong" purely-geometric effects at dN/dy~100.

Trajectum framework
Ratio 20Ne+20Ne /16O+16O

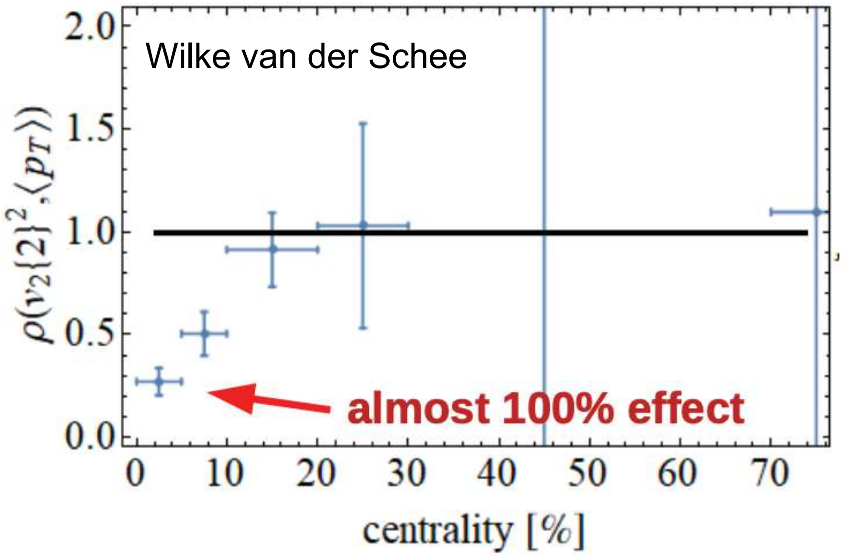

Imaging strong shape evolution of $^{144-154}$Sm isotopic chain

Transition from nearly-spherical to well-deformed nuclei when size increase by less than 7%. Using HI to access the multi-nucleon correlations leading to such shape evolution, as well as dynamical β_3 and β_4 shape fluctuations.

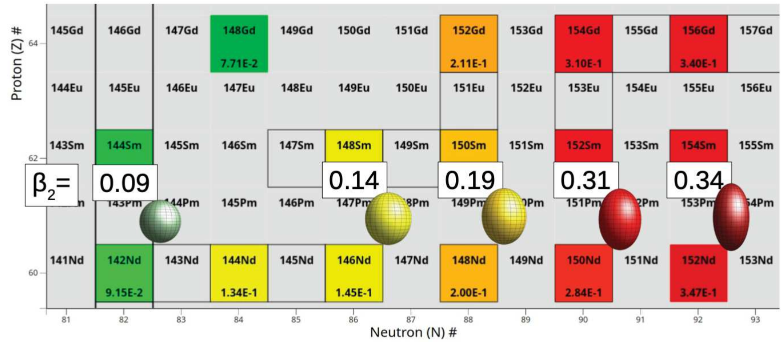

$$\left\langle \epsilon_2^2 \right\rangle = a' + b' \beta_2^2$$
$$\left\langle v_2^2 \right\rangle = a + b \beta_2^2$$

In central collisions

$$a' = \left\langle \varepsilon_2^2 \right\rangle_{|\beta_2=0} \propto 1/A$$
$$a = \left\langle v_2^2 \right\rangle_{|\beta_2=0} \propto 1/A$$

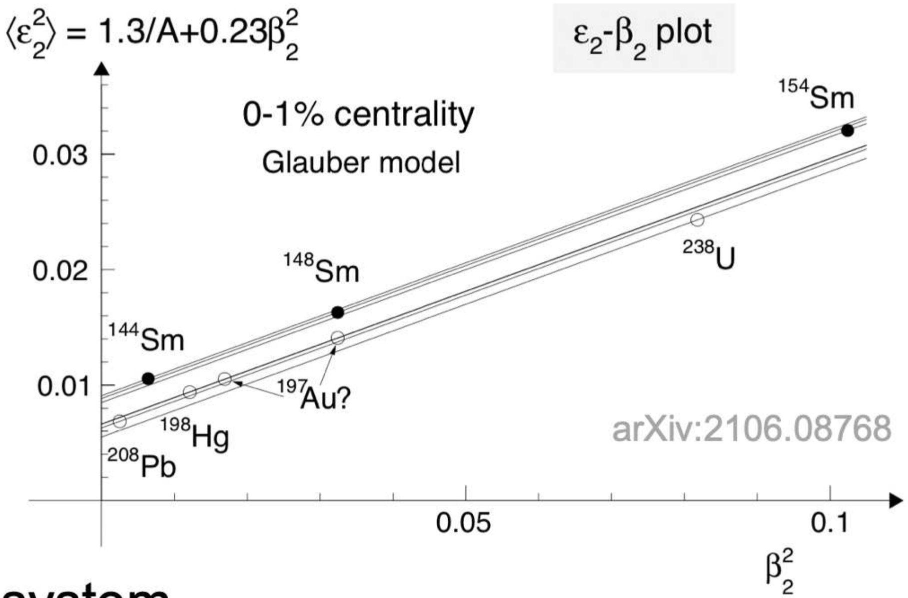

b’, b are ~ independent of system

Systems with similar A fall on the same curve.

Fix a and b with two isobar systems with known β_2, then make predictions for the third one

Neutron skin in high-energy collisions

The famous PREX and CREX has tension with theory and previous exp. Indicate a larger L value.

$$\Delta r_{\mathrm{np,Pb}} = 0.28 \pm 0.07\mathrm{fm}$$
$$\Delta r_{\mathrm{np,Ca}} = 0.14 \pm 0.03\mathrm{fm}$$

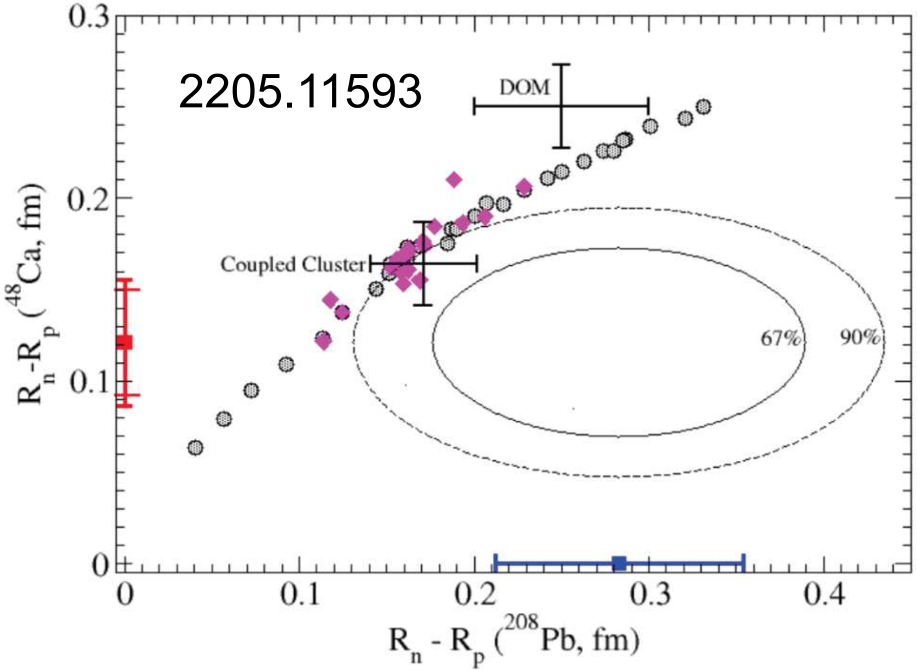

- Access the difference of neutron skin by comparing 40Ca+40Ca and 48Ca+48Ca

$$\Delta_{\mathrm{np}}\left({}^{48}\mathrm{Ca}\right) - \Delta_{\mathrm{np}}\left({}^{40}\mathrm{Ca}\right) \simeq \Delta_{\mathrm{np}}\left({}^{48}\mathrm{Ca}\right)$$

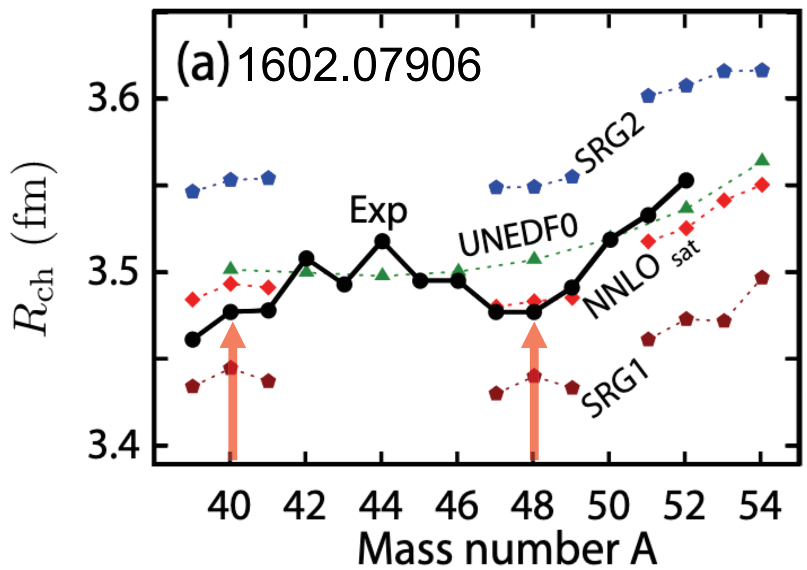

Neutron skin for 208Pb

- Extract skin of 208Pb in UPC or by comparing with 197Au

Photo-nuclear in UPC

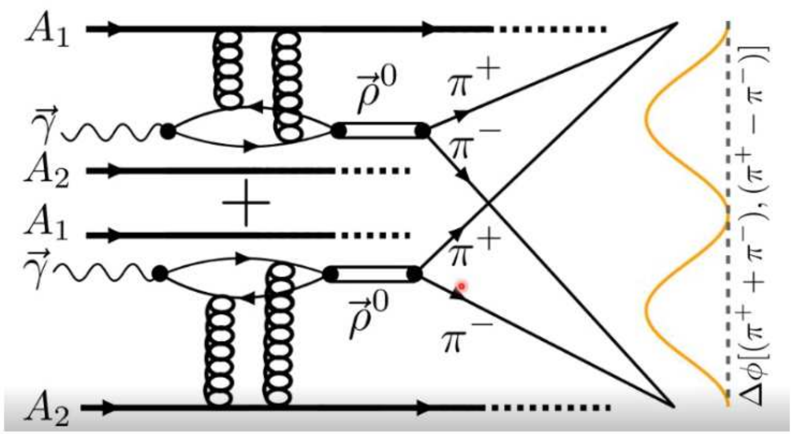

Neutron skin: STAR: 2204.01625

$0.44 \pm 0.05(\text{stat.}) \pm 0.08(\text{syst.})$ fm for ^{238}U

$0.17 \pm 0.03(\text{stat.}) \pm 0.08(\text{syst.})$ fm for ^{197}Au

reaction-plane elliptic flow

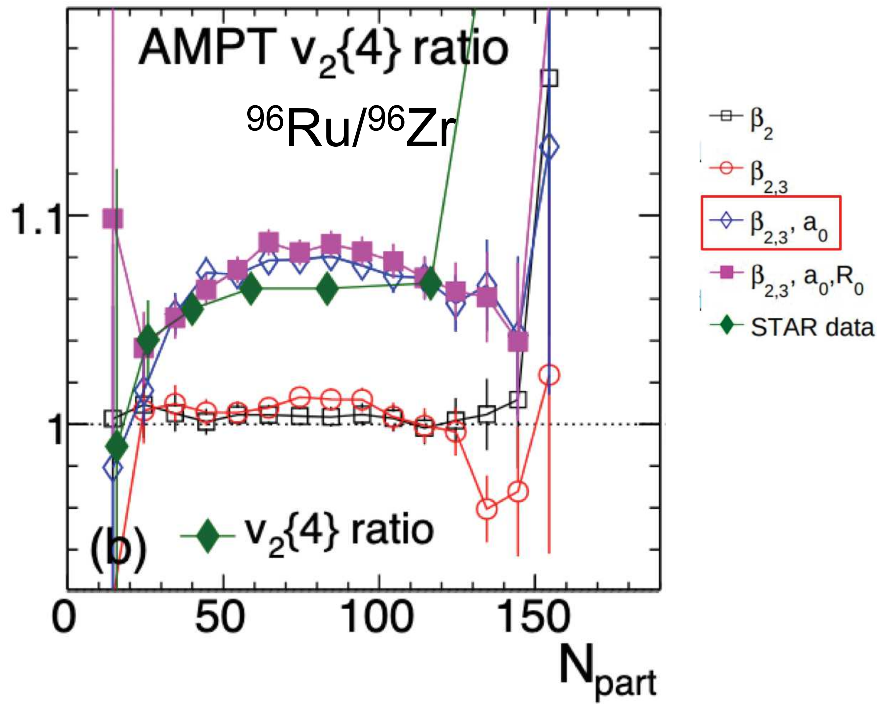

2206.10449

Shape-fluctution or shape-mixing

- Further explore connections between NS and HI, more observables
  - More case studies with Ru/Zr, Au/U, Pb/Xe. cancel most final state effect
  - Shape fluctuations and shape coexistence

quadrupole operator $\hat{Q}$

$$\begin{cases} \langle \beta^2 \rangle = \dfrac{16\pi^2}{9A^2R_0^4}\left\langle \hat{Q}^2 \right\rangle \\ \sigma^2(\langle\beta^2\rangle)/\langle\beta^2\rangle = \sigma^2\left(\langle\hat{Q}^2\rangle\right)/\langle\hat{Q}^2\rangle \end{cases}$$

2-p correlation

4-p correlation

Shape coexistence

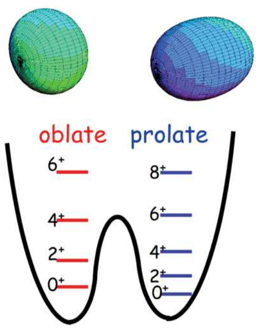

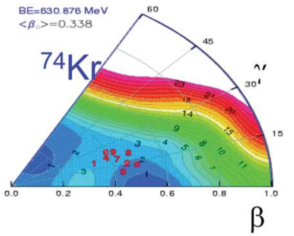

1906.07542

$$\begin{cases} \langle \cos 3\gamma \rangle = -\sqrt{\dfrac{7}{2}}\dfrac{\left\langle \hat{Q}^3 \right\rangle}{\left\langle \hat{Q}^2 \right\rangle^{3/2}} \\ \dfrac{\sigma^2(\cos 3\gamma)}{\langle\cos 3\gamma\rangle^2} = \dfrac{\sigma^2\langle\hat{Q}^3\rangle}{\langle\hat{Q}^3\rangle^2} + \dfrac{9}{4}\dfrac{\sigma^2\langle\hat{Q}^2\rangle}{\langle\hat{Q}^2\rangle^2} - 3\dfrac{\langle\hat{Q}^5\rangle - \langle\hat{Q}^3\rangle\langle\hat{Q}^2\rangle}{\langle\hat{Q}^3\rangle\langle\hat{Q}^2\rangle} \end{cases}$$

3-p correlation

6-p correlation

Heavy ion observables:

$$\frac{\left\langle \varepsilon_2^2 \right\rangle}{\frac{3}{4\pi}\beta_2^2} \Longleftrightarrow \frac{\left\langle \varepsilon_2^4 \right\rangle - 2\left\langle \varepsilon_2^2 \right\rangle^2}{-\frac{9}{56\pi^2}\beta_2^4}$$

$$\frac{\left\langle \varepsilon_2^2(\delta d_\perp/d_\perp) \right\rangle}{-\frac{3\sqrt{5}}{112\pi^{3/2}}\cos(3\gamma)\beta_2^3} \Longleftrightarrow \frac{\left(\left\langle \varepsilon_2^6 \right\rangle - 9\left\langle \varepsilon_2^4 \right\rangle\left\langle \varepsilon_2^2 \right\rangle + 12\left\langle \varepsilon_2^2 \right\rangle^3\right)/4}{\frac{27(373-25\cos(6\gamma))}{32\times 8008\pi^3}\beta_2^6}$$

Summary

- Precision QGP initial condition via constraints from both NS input and HI observables➔ Improve the extraction of QGP properties.
- Understanding how initial condition respond to NS in turn allow us to probe novel nuclear structure properties and compliment low-energy experiments
- Identify interesting isobar species across nuclear chart to map out initial condition from small to larger system (250 stable isotopes, 141 isobar pairs or triplets)

$$e(x,y) \propto \left(\frac{T_A^p + T_B^p}{2}\right)^{q/p}$$

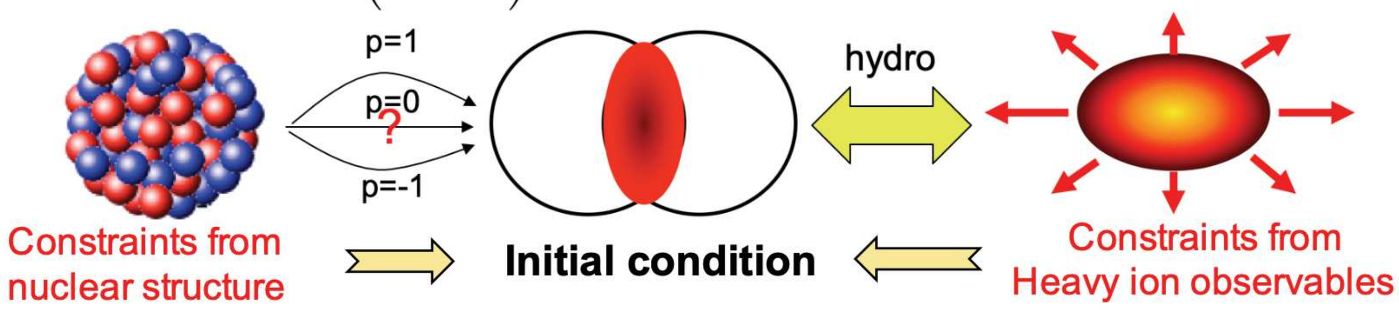

PROGRAM

JANUARY 23 - FEBRUARY 24, 2023

Intersection of nuclear structure and high-energy nuclear collisions (23-1a)

INSTITUTE for NUCLEAR THEORY

Organizers:
Giuliano Giacalone (Heidelberg)
Jiangyong Jia (Stony Brook & BNL)
Dean Lee (Michigan State & FRIB)
Matt Luzum (São Paulo)
Jaki Noronha-Hostler (Urbana-Champaign)
Fuqiang Wang (Purdue)

arXiv:2102.08158

A	isobars	A	isobars	A	isobars
36	Ar, S	106	Pd, Cd	148	Nd, Sm
40	Ca, Ar	108	Pd, Cd	150	Nd, Sm
46	Ca, Ti	110	Pd, Cd	152	Sm, Gd
48	Ca, Ti	112	Cd, Sn	154	Sm, Gd
50	Ti, V, Cr	113	Cd, In	156	Gd, Dy
54	Cr, Fe	114	Cd, Sn	158	Gd, Dy
64	Ni, Zn	115	In, Sn	160	Gd, Dy
70	Zn, Ge	116	Cd, Sn	162	Dy, Er
74	Ge, Se	120	Sn, Te	164	Dy, Er
76	Ge, Se	122	Sn, Te	168	Er, Yb
78	Se, Kr	123	Sb, Te	170	Er, Yb
80	Se, Kr	124	Sn, Te, Xe	174	Yb, Hf
84	Kr, Sr, Mo	126	Te, Xe	176	Yb, Lu, Hf
86	Kr, Sr	128	Te, Xe	180	Hf, W
87	Rb, Sr	130	Te, Xe, Ba	184	W, Os
92	Zr, Nb, Mo	132	Xe, Ba	186	W, Os
94	Zr, Mo	134	Xe, Ba	187	Re, Os
96	Zr, Mo, Ru	136	Xe, Ba, Ce	190	Os, Pt
98	Mo, Ru	138	Ba, La, Ce	192	Os, Pt
100	Mo, Ru	142	Ce, Nd	198	Pt, Hg
102	Ru, Pd	144	Nd, Sm	204	Hg, Pb
104	Ru, Pd	146	Nd, Sm		

Test scaling in AMPT

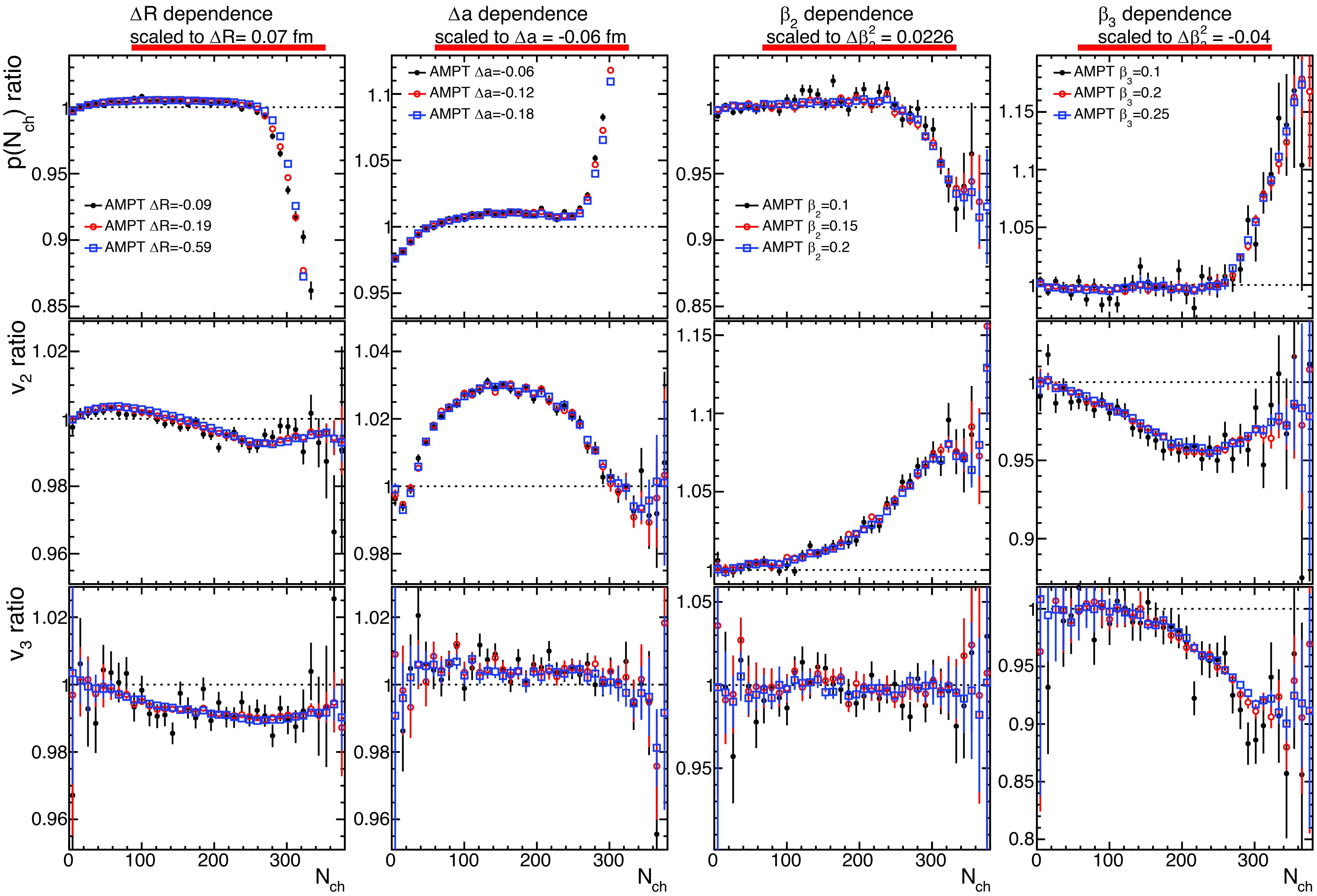

Verifies the relation: $1 + c_1\Delta\beta_2^2 + c_2\Delta\beta_3^2 + c_3\Delta a + c_4\Delta R$